

# Alpine metamorphism of pelitic schists in the south-east Tauern Window, Austria

Autor(en): **Droop, G.T.R.**

Objektyp: **Article**

Zeitschrift: **Schweizerische mineralogische und petrographische Mitteilungen  
= Bulletin suisse de minéralogie et pétrographie**

Band (Jahr): **61 (1981)**

Heft 2-3

PDF erstellt am: **21.07.2024**

Persistenter Link: <https://doi.org/10.5169/seals-47140>

## **Nutzungsbedingungen**

Die ETH-Bibliothek ist Anbieterin der digitalisierten Zeitschriften. Sie besitzt keine Urheberrechte an den Inhalten der Zeitschriften. Die Rechte liegen in der Regel bei den Herausgebern.

Die auf der Plattform e-periodica veröffentlichten Dokumente stehen für nicht-kommerzielle Zwecke in Lehre und Forschung sowie für die private Nutzung frei zur Verfügung. Einzelne Dateien oder Ausdrucke aus diesem Angebot können zusammen mit diesen Nutzungsbedingungen und den korrekten Herkunftsbezeichnungen weitergegeben werden.

Das Veröffentlichen von Bildern in Print- und Online-Publikationen ist nur mit vorheriger Genehmigung der Rechteinhaber erlaubt. Die systematische Speicherung von Teilen des elektronischen Angebots auf anderen Servern bedarf ebenfalls des schriftlichen Einverständnisses der Rechteinhaber.

## **Haftungsausschluss**

Alle Angaben erfolgen ohne Gewähr für Vollständigkeit oder Richtigkeit. Es wird keine Haftung übernommen für Schäden durch die Verwendung von Informationen aus diesem Online-Angebot oder durch das Fehlen von Informationen. Dies gilt auch für Inhalte Dritter, die über dieses Angebot zugänglich sind.

## **Alpine Metamorphism of Pelitic Schists in the South-East Tauern Window, Austria**

by *G. T. R. Droop*<sup>1</sup>

### **Abstract**

Mineral parageneses and textures are described from pelitic schists of the Pennine Zone exposed in the south-east Tauern Window, Austria.

The metamorphic history of the metapelites is summarised. AFM-mineral assemblages in most rocks equilibrated close to the thermal peak of the 35–40 my Alpine regional metamorphism after major Alpine penetrative deformation had ceased, but relict pre-Alpine regional and contact metamorphic assemblages are recognised in schists of the Pennine Basement Complex.

Representative mineral analyses are presented. Garnets from both Inner Schieferhülle (Basement) and Peripheral Schieferhülle (Cover) schists are zoned but no zoning was detected in other AFM minerals. Mg/Mg + Fe ratios of coexisting AFM-minerals increase in the order: garnet < staurolite < chloritoid < biotite < chlorite.

AFM phase relations are analysed using THOMPSON (1957) projections. Three groups of compatible high-variance AFM assemblages are distinguished; the groups are related to one another by crossed tie-line relationships. Explanations are suggested for the low-variance AFM assemblages abundant in one part of the area.

The spatial variation in Alpine peak metamorphic P-T conditions is examined by mapping metamorphic zones in muscovite + quartz-bearing metapelites. Three zones are recognised on the basis of critical AFM-mineral assemblages: (i) a staurolite + biotite zone, which coincides roughly with the area of greatest basement updoming, (ii) a garnet + chlorite zone, which covers mostly structurally high rock units exposed near the edge of the Window, and (iii) a thin, wedge-shaped chloritoid + biotite zone between the other two. An ill-defined garnet + staurolite + chlorite subzone occurs in the highgrade part of the garnet + chlorite zone, but only where the chloritoid + biotite zone is missing. The isograds separating these zones and subzones are modelled on univariant reactions involving garnet, staurolite, chloritoid, biotite, chlorite, muscovite, quartz and H<sub>2</sub>O-rich fluid. The relative equilibrium P-T positions of these model reactions are located using published metapelite petrogenetic grids; they indicate that Alpine metamorphic temperatures increased with structural depth towards the central part of the eastern Tauern Window, but also imply either (i) the existence of an isothermal pressure gradient at the peak of metamorphism, or (ii) that the pressure at any isotherm was essentially constant, but that the P-T positions of the model univariant reactions are highly sensitive to variations in bulk rock concentrations of non-AFM components such as Ca or Mn. As yet there is insufficient evidence to choose between these hypotheses. The existence of an isothermal pressure gradient would imply that the thermal structure of the south-east Tauern Window was laterally inhomogeneous during the prograde part of the Alpine metamorphic cycle,

---

<sup>1</sup> Department of Geology and Mineralogy, Parks Road, Oxford OX1 3PR.

and that Alpine metamorphism in this area cannot be modelled by a single one-dimensional thermal model.

Mineral textures in selected rocks are examined to ascertain the time relations of growth of AFM-minerals and to identify the actual reactions by which they formed. Assemblages developed as the result of both continuous and discontinuous reactions. Some of the latter can be equated with the model isograd reactions. More than one sequence of reactions operated in metapelites of similar AFM compositions.

### Introduction

The purpose of this paper is to examine, qualitatively, the spatial variation in Alpine metamorphic temperatures and pressures over part of the south-east Tauern Window. The need for this study has arisen partly as the result of recent attempts by OXBURGH and TURCOTTE (1974), BICKLE et al. (1975) and ENGLAND (1978) to assess the thermal causes of the 35 my regional metamorphism in the Tauern Window without detailed knowledge of the metamorphic conditions. The study is restricted to metapelites which, although poorly represented in the area of interest show a very varied mineralogy and a distinct metamorphic zonation, unlike the more common lithologies. Since metapelitic mineral assemblages have been widely used as both qualitative and quantitative indicators of metamorphic grade, a paragenetic study of the south-east Tauern metapelites should therefore enable one to compare directly the Alpine metamorphism in this area with the metamorphism in well characterised terrains such as the Scottish Caledonides.

The area examined lies immediately north of the river Möll and includes the towns of Mallnitz, Obervellach and Kolbnitz. Its location is shown in fig. 1.

#### Abbreviations used in the text and tables

P	pressure	my	million years before present
P <sub>tot</sub>	lithostatic pressure	kb	kilobars
P <sub>H<sub>2</sub>O</sub>	water pressure	a <sub>H<sub>2</sub>O</sub>	activity of water
T	temperature	μ <sub>H<sub>2</sub>O</sub>	chemical potential of water
acc	accessory minerals	ilm	ilmenite
as	Al <sub>2</sub> SiO <sub>5</sub> mineral	ky	kyanite
biot	biotite	mt	magnetite
chl	chlorite	musc	muscovite
cord	cordierite	par	paragonite
ctd	chloritoid	plag	plagioclase
ep	epidote	qz	quartz
gt	garnet	st	staurolite

GD 1197, C 523, RN 247, etc. rock sample numbers

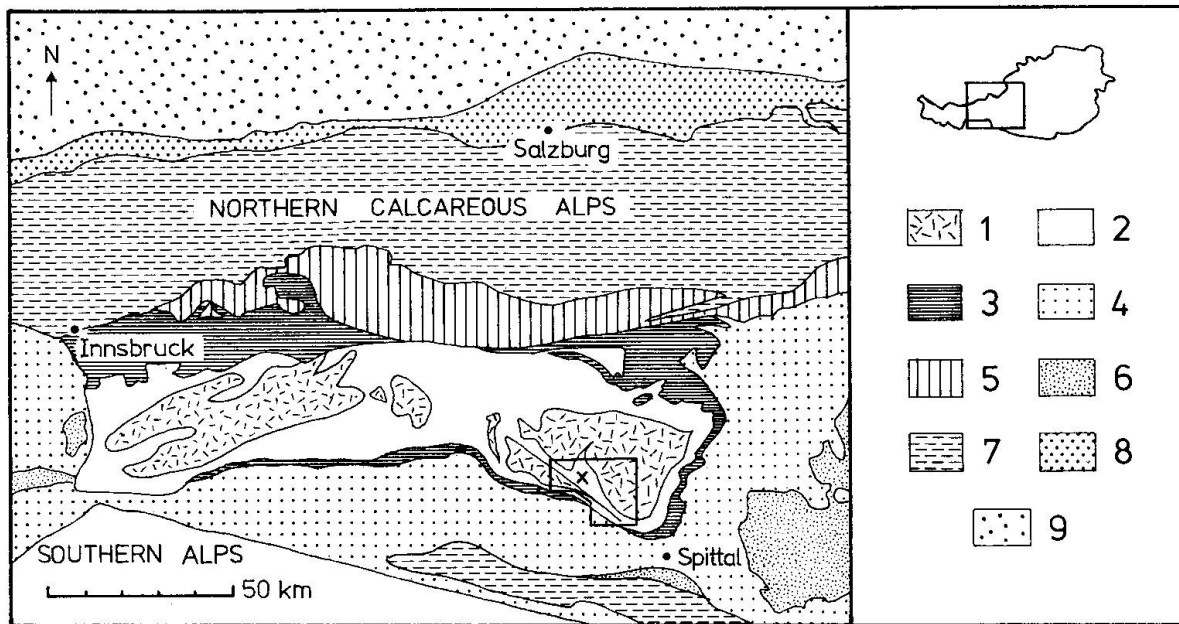


Fig. 1 Sketch map of the Eastern Alps.

1. Pennine Basement Complex. 2. Peripheral Schieferhülle. 3. Lower East Alpine Sheet. 4. Altkristallin. 5. Grauwackenzone. 6, 7. Sedimentary cover of the Altkristallin sheet. 8. Flysch and Helvetic zones. 9. Molasse. X. Area examined in this paper.

Parts of it have been mapped by ANGEL and STABER (1952), EXNER (1962, 1964), CLIFF et al. (1971) and DROOP (1979). CLIFF et al. (1971) also made a preliminary investigation of the metamorphism.

### Geology

The rocks which outcrop within the Tauern Window belong to the Pennine Zone; they are tectonically overlain by the Austro-Alpine thrust sheets which outcrop around the Tauern Window (fig. 1). The Pennine Zone of the Eastern Alps can be subdivided into the following three main structural units (in the terminology of CLIFF et al. 1971):

1. Inner Schieferhülle: Polymetamorphic schists and gneisses which show evidence of at least one phase of both pre-Alpine regional metamorphism and pre-Alpine deformation.

2. Zentralgneis: Large volumes of plutonic granite, adamellite, tonalite and quartz-monzonite, some of which are clearly intrusive into the Inner Schieferhülle (CLIFF et al., 1971). The Zentralgneis has yielded Rb/Sr whole rock ages of ca. 255 my for leucogranites (LAMBERT, 1974; BESANG et al., 1968; JÄGER et al., 1969; CLIFF, 1968, 1971; SATIR, 1974) and of  $279 \pm 9$  my for granodiorites (HAWKESWORTH, 1976).



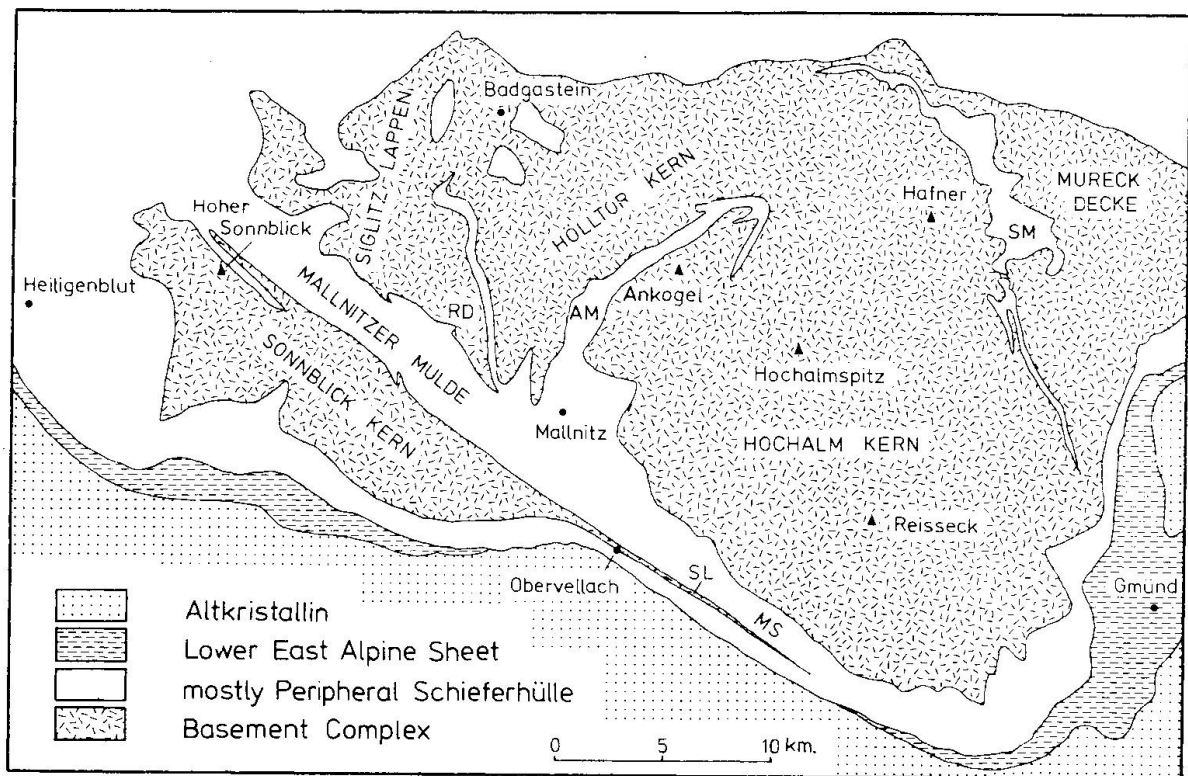


Fig. 2 Sketch map of the south-east Tauern Window.

AM. Ankogel Mulde, MS. Mölltal Schieferhülle, RD. Romate Decke, SL. Sonnblick lamella, SM. Silbereck Mulde.

Together, these two subdivisions form the pre-Alpine Basement Complex. Zentralgneis is much more abundant than Inner Schieferhülle, the latter forming occasional bands and screens between masses of plutonic rock. Basement rocks tend to outcrop in "gneiss domes" towards the central parts of the south-east Tauern Window (figs. 1 and 2).

3. *Peripheral Schieferhülle*: Intensely deformed Mesozoic metasediments and metavolcanics. Typical lithologies include calc-schist, graphitic mica-schist, marble, dolomite, pelitic schist, epidote-amphibolite and serpentinite. Discordant intrusive granites are absent. *Peripheral Schieferhülle* rocks tectonically overlie those of the Basement Complex, and are themselves tectonically overlain by the Austro-Alpine nappes. Consequently, they tend to outcrop in the marginal parts of the Window and in tight synformal depressions between the gneiss domes.

Two widespread phases of Alpine penetrative deformation have been recognised in the Tauern Window (BICKLE and HAWKESWORTH, 1978; HOLLAND, 1979; DROOP, 1979). The first of these,  $D_1^1$  (this author's notation) affected only the *Peripheral Schieferhülle* and the structurally highest parts of the Basement Complex; it is generally ascribed to the main phase of thrusting of the semi-rigid upper Austro-Alpine nappe over the Pennine Zone. The second,  $D_2^2$  de-

formed Pennine units at all structural levels, and was generally less intense than  $D_a^1$ .

In the Tauern Window, the effects of pre-Alpine metamorphism are confined to the Inner Schieferhülle. The first phase of regional metamorphism to affect the Zentralgneis was the 35 mybp greenschist to amphibolite facies event; this also *appears* to be the first event to have affected much of the Peripheral Schieferhülle. Relict eo-Alpine eclogite and blueschist assemblages are, however, preserved locally in the Peripheral Schieferhülle of the Central Tauern (MILLER, 1974, 1977; HOLLAND, 1979) but are absent from the area of study. Eo-Alpine high-pressure assemblages may once have been widely developed in the south-east Tauern, though if so they must have been thoroughly recrystallised and overprinted during the prograde stages of late Alpine metamorphism. Almost all Inner Schieferhülle rocks show evidence of partial late Alpine recrystallisation.

CLIFF et al. (1971) were the first workers to examine the metamorphism in the area of interest. They established the existence of an albite-oligoclase isograd north of the Mölltal separating an area of low Alpine metamorphic grade to the south-west from an area of higher grade to the north-east.

#### **Distribution and petrography of pelitic schists in the South-East Tauern**

Pelitic and semi-pelitic schists were mapped together as «mica-schists» by EXNER (1964), CLIFF et al. (1971) and DROOP (1979). Mica-schists occur in both Inner and Peripheral Schieferhülle, but form only a small part of either. Within the mica-schists, the proportion of truly pelitic bands in otherwise semi-pelitic and feldspathic schists is variable but generally small, particularly in the Inner Schieferhülle. Many Inner Schieferhülle schists have been heavily injected by Zentralgneis granite and merit the name migmatite.

##### **(i) Inner Schieferhülle metapelites:**

Inner Schieferhülle metapelites tend to be compact, fine-grained silvery-grey rocks rich in muscovite and poor in biotite and quartz. Some, particularly the varieties with more than average quartz, have a well-developed mica-schistosity cross-cut by flakes of mica in random orientation; in others, the mica fabric is largely decussate. Large (< 4 mm) strained, partially recrystallised muscovites occur in some migmatitic varieties.

Two populations of garnet are commonly found in the same rock: large ( $\frac{1}{2}$ –15 mm) zoned porphyroblasts, and small (<  $\frac{1}{2}$  mm) subhedral «pin-prick» grains. The porphyroblasts generally consist of large, well-rounded cores sepa-

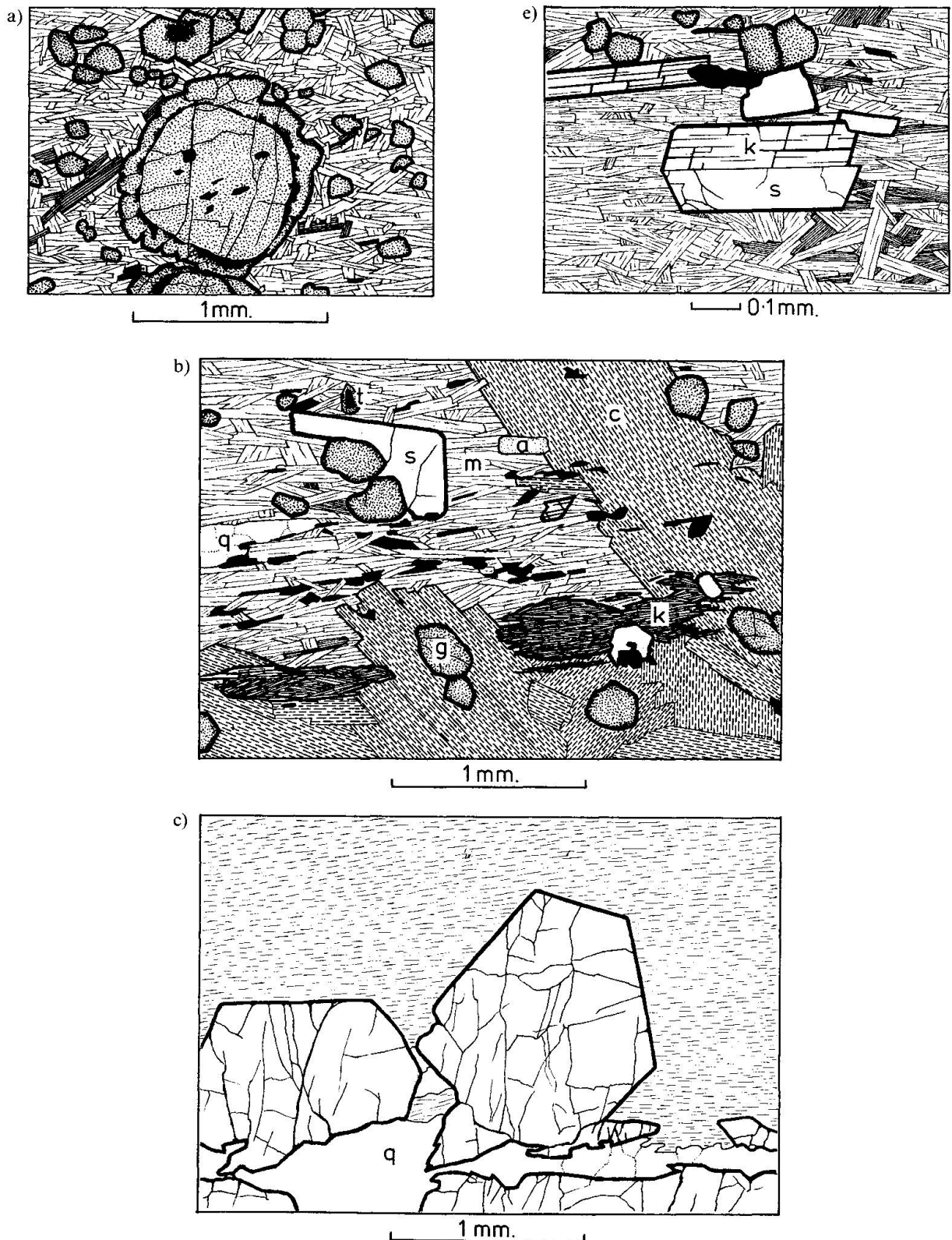
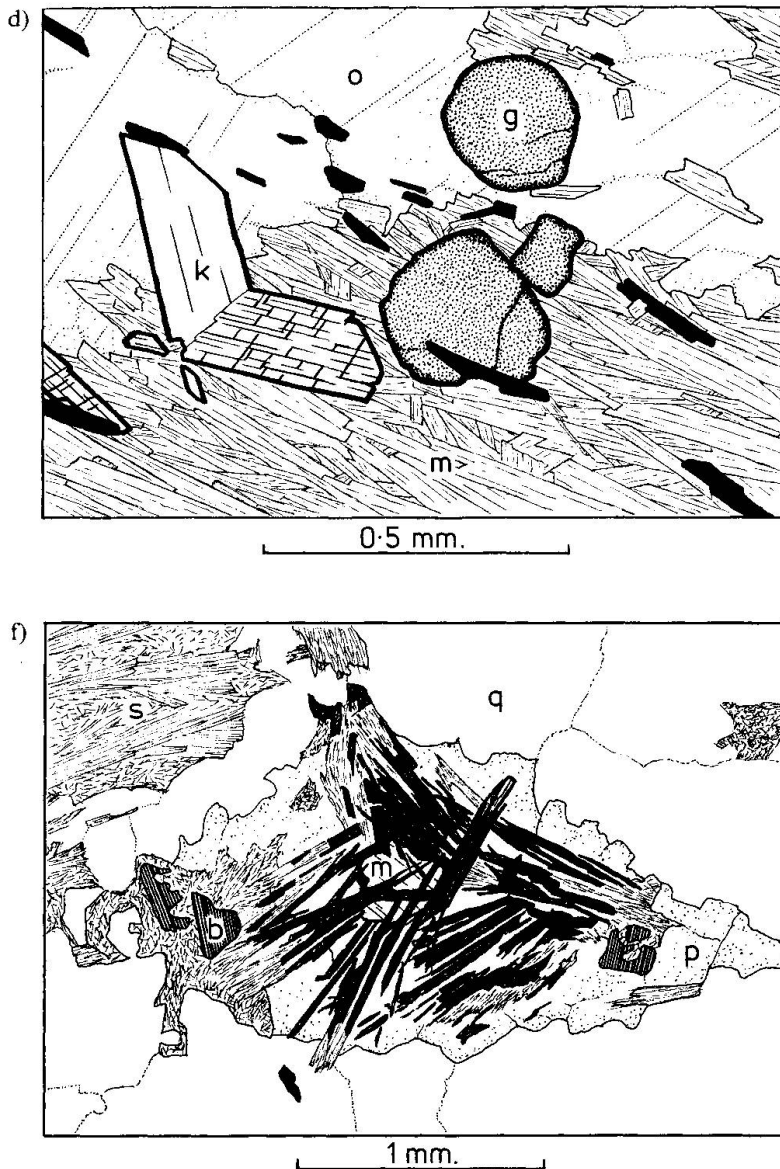


*Fig. 3* Mineral textures in Inner Schieferhülle metapelites.

a) Zoned garnet porphyroblast (with pre-Alpine core and Alpine rim) and Alpine «pin-prick» garnets in a decussate muscovite and biotite matrix. GD209 a.

b) Large chlorite porphyroblast (c), overgrowing garnet (g), ilmenite, staurolite and acicular kyanite (k), and cutting



across aligned muscovite flakes (m). A euhedral staurolite (s) partially encloses garnets. Quartz (q), apatite (a) and tourmaline (t) are also shown. GD 208 d.

c) Euhedral staurolite porphyroblasts cutting across schistosity in fine grained monomineralic paragonite which locally contacts quartz (q). GD 209 a.

d) Ragged oligoclase porphyroblasts (o) replacing muscovite (m) and overgrowing ilmenite and post-tectonic «pin-prick» garnets (g) and kyanite (k). GD 208 d.

e) Parallel growth of staurolite (s) and kyanite (k), with garnet, muscovite, biotite and ilmenite. GD 209 a.

f) Partly sericitised kyanite pseudomorphs after sillimanite surrounding a relict muscovite (m), in a matrix of quartz (q), plagioclase (p), biotite (b) and sericite (s). RN 247.

rated sharply from thin lobate rims of lower relief, commonly dusted with opaque material (fig. 3 a). The rims are about as wide as the «pin-prick» grains and probably represent the same growth stage.

Where present, staurolite and kyanite generally occur as subhedral prisms which overgrow »pin-prick« garnets and cut across any existing mica schistosi-

ty in random orientation (fig. 3b, 3c and 3d). In addition to discrete kyanite prisms, some samples contain lenticular aggregates (2 x 0.5 mm) of aligned kyanite needles (fig. 3b). Large, bent kyanites, partially replaced by chlorite, muscovite and plagioclase have been found in two rocks (C 523, GD 652).

Paragonite has been identified in four Inner Schieferhülle metapelites. In GD 465b and the bulk of GD 209a, decussate muscovite and paragonite are present in roughly equal proportions. In a 1 cm wide band in GD 209a, euhedral prisms of staurolite and kyanite are set in a monomineralic matrix of fine-grained, schistose paragonite (fig. 3c). In the aluminous quartzite GD 208e, quartz and oligoclase form polygonal grains elongated parallel to the muscovite and paragonite schistosity. In this rock, plagioclase is clearly in equilibrium with the micas, but in other Inner Schieferhülle metapelites, the plagioclase, where present, invariably forms large (< 1 cm) patches overgrowing garnet, staurolite and kyanite and replacing white-mica (fig. 3d). Radiating sheaves of chlorite also enclose the AFM orthosilicates (fig. 3b) and is assumed to be retrogressive.

Ilmenite is the characteristic ore mineral, but is sometimes accompanied by magnetite. It has a platy habit and its texture mimics that of the surrounding mica (figs. 3b and 3d).

#### (ii) Peripheral Schieferhülle metapelites:

The majority of Peripheral Schieferhülle metapelites contain numerous 1 to 10 mm porphyroblasts of garnet set in a fine-grained, silvery, schistose matrix of white-mica with or without chlorite and/or biotite. Other conspicuous porphyroblast minerals, which may be present in various combinations with or without garnet, include plagioclase, chloritoid, biotite, magnetite and ilmenite. Staurolites and kyanites are generally too small to be identified in hand specimen. Many of the petrographic features of these schists are described in the section headed "Reaction Textures" but a few generalisations are given here.

Several textural types of garnet have been found. In quartz-rich schists they tend to have poorly developed crystal faces and numerous quartz inclusions, while those in fine-grained quartz-poor schists are generally euhedral. In either case, the garnets may have grown before, during or after the development of the  $D_a^2$  mica-schistosity, giving rise to a variety of forms: rounded with quartz pressure-shadows, cross-cutting (e.g. fig. 4a), sigmoidal, etc. Ilmenite, chloritoid, graphite, quartz, epidote and tourmaline are commonly found as isolated or aligned inclusions within garnet. Inclusion trails may be straight, folded, sigmoidal, convergent, and either concordant or discordant to the matrix schistosity.

Where present, biotite forms reddish-brown flakes either lying in or cutting across the  $D_a^2$  muscovite schistosity. Both types may be found in the same rock



(e.g. fig. 4c). In a few specimens, biotite is partially altered to chlorite with anomalous blue interference colours, but in many, abundant chlorite with brownish interference colours has grown parallel to the  $D_a^2$  schistosity and appears to be primary.

Chloritoid forms blocky plate up to 2 mm across with various relationships with the mica fabric. Pre- and syn-tectonic varieties are common, but post-tectonic chloritoid appears to be confined to schists of the chloritoid + biotite zone (p. 263 and fig. 4c). In some staurolite-bearing rocks, the only chloritoid present occurs as inclusions within garnet.

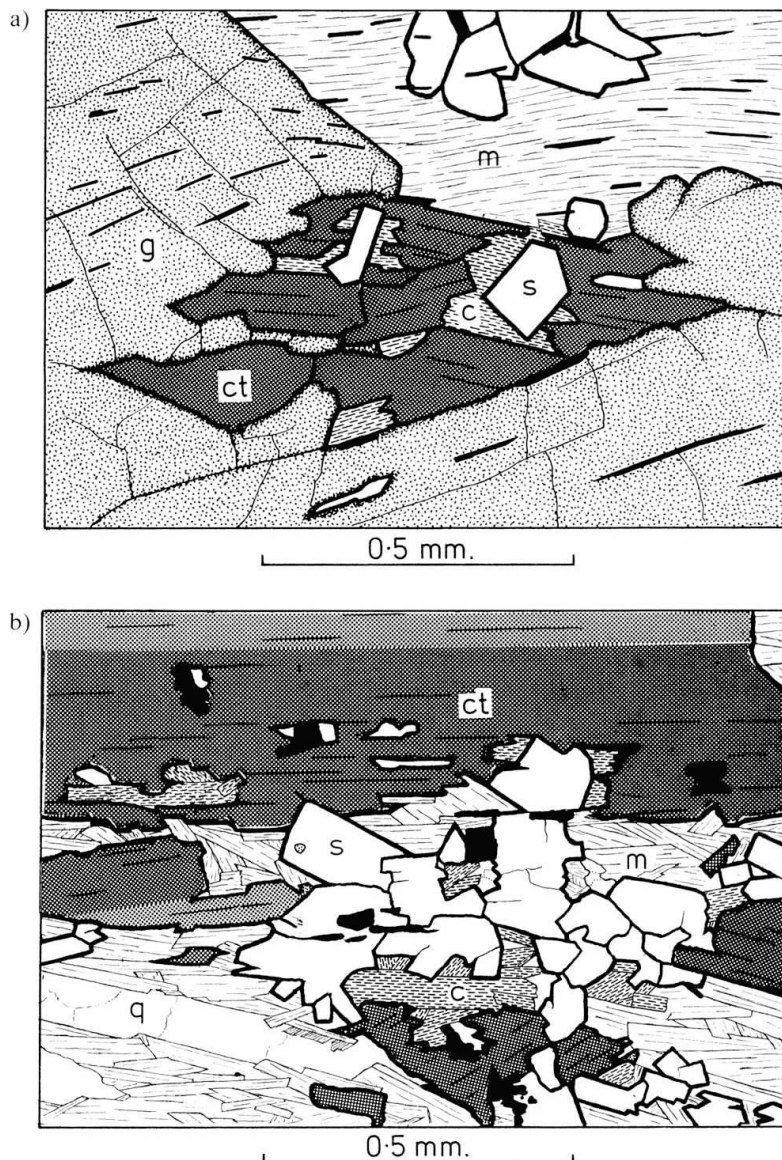


Fig. 4 Mineral textures in Peripheral Schieferhülle metapelites.

a) Staurolite (s) and chlorite (c) growing at the expense of chloritoid (ct) partially enclosed by garnet (g). Staurolite and garnet cut across a muscovite (m) schistosity and enclose aligned ilmenite plates. GD 43 b.

b) Staurolite (s), chlorite (c) and magnetite growing from chloritoid (ct), with muscovite (m) and quartz (q). GD 308 c.

The staurolite in Peripheral Schieferhülle metapelites are pale compared with these from other terrains. They are mustard coloured in hand-specimen and pale watery-yellow in thin section. They generally form cross-cutting, euhedral, inclusion-free prisms often with knee-twins, and in many instances appear to have grown at the expense of either chloritoid (figs. 4a and 4b) or garnet (fig. 4d). Kyanite was found in four Peripheral Schieferhülle metapelites. Its textural relationships with the mica schistosity are unclear, but seem to mimic those of staurolite. Some of the kyanite in GD 18 and GD 438 has been replaced by plagioclase.

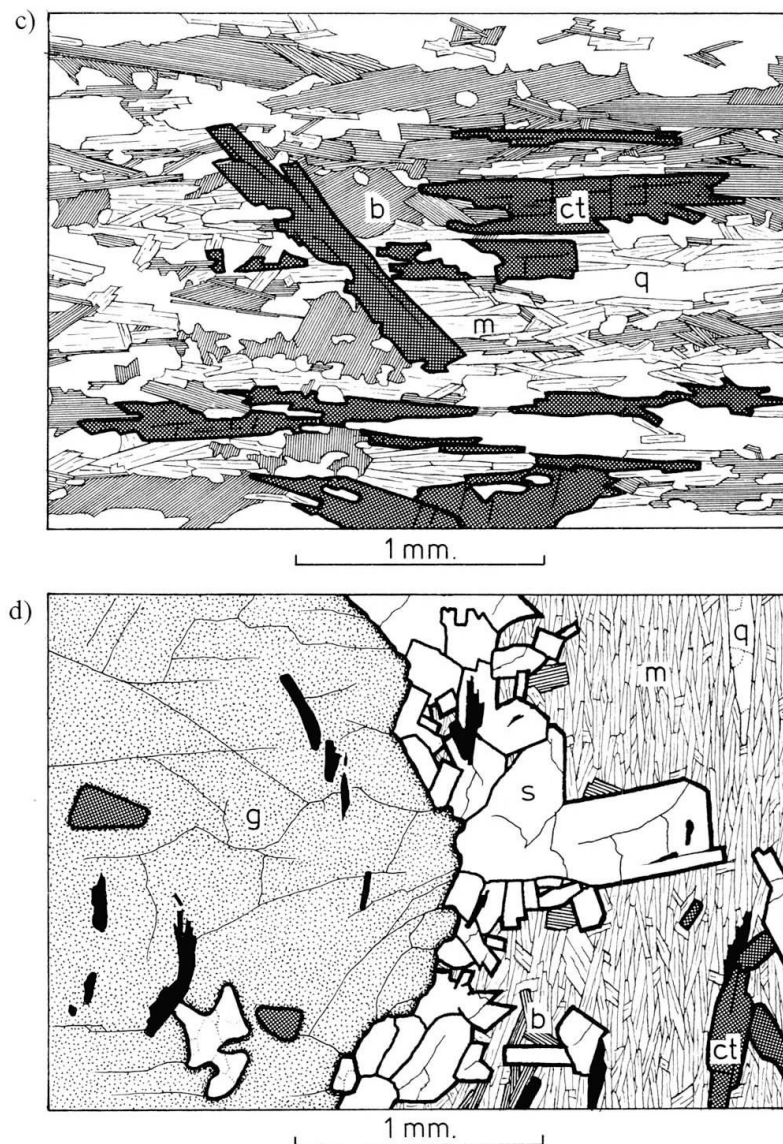


Fig. 4 (cont'd)

c) Chloritoid(ct) apparently in equilibrium with biotite(b), muscovite(m) and quartz(q). GD 168b.

d) Reaction rim of euhedral, post-tectonic staurolite crystals (s) and biotite (b) surrounding a porphyroblast of garnet (g). Chloritoid (ct), ilmenite and quartz (q) coexist with muscovite (m) but also occur as inclusions within garnet. GD 1296.

Rounded, rotated albite porphyroblasts occur in some of the less aluminous metapelites. More common, however, are post-tectonic patchy porphyroblasts of oligoclase-andesine (< 7 mm) which appear to have replaced muscovite; they occur either individually or as overgrowths on albite cores and occasionally enclose random biotite, staurolite, etc. Paragonite has been identified in three Peripheral Schieferhülle schists; in all of them it has a fine-grained schistose texture.

The characteristic ore mineral is magnetite which forms octahedra or skeletal crystals up to 1 mm. Ilmenite is less common, and usually forms plates aligned in the schistosity (fig. 4a).

The mineral assemblages of some representative metapelites from the south-east Tauern are listed in tables 1 and 2.

### Recognition of alpine and pre-alpine mineral assemblages

Rocks of the Basement Complex outcrop over a large part of the area of interest (fig. 1 and 2). In order to study the Alpine metamorphic imprint in this area, it is therefore necessary to identify the pre-Alpine components of mineral assemblages in the polymetamorphic pelitic schists of the Inner Schieferhülle so that they are not erroneously included in a paragenetic study of Alpine metamorphism.

Table 1 Mineral assemblages of representative Inner Schieferhülle metapelites. Mineral name abbreviations as in text.

A: apatite, R: rutile, T: tourmaline, Z: zircon, X: essential mineral, O: accessory mineral.

Superscripts: H: Hercynian, L: late-stage porphyroblasts, S: pseudomorphs after sillimanite, 2: two generations.

	GT	ST	KY	CTD	CHL	BIOT	MUSC	PAR	EP	QZ	PLAG	MT	ILM	ACC	LOCALITY
GARNET + CHLORITE ZONE															
GD 1192		X <sup>2</sup>			O	X	X			X	X		O	AR	Hochalmblick, Seebach Tal.
GD 1230C		X <sup>2</sup>			O	X	X		O	X	X		O	A	Woisgen Scharte.
GD 652		X <sup>H</sup>	O <sup>H</sup>	X <sup>H</sup>	X	X	X		O	X	X	O	O	AR	Koast Wald, Mallnitz.
STAUROLITE + BIOTITE ZONE															
GD 74C		X			O <sup>L</sup>	X	X		O	X	X <sup>L</sup>		O	AR	N. side Dösender See.
GD 80A		X	X	X	X <sup>L</sup>	X	X			X	X <sup>L</sup>		O	T	S. shore Dösender See.
GD 80B					X	X	X		O	X	X <sup>L</sup>				S. shore Dösender See.
GD 82		X	X		X <sup>L</sup>	X	X		O	X	X <sup>L</sup>	O	O	A	Seeschartl.
GD 208D		X	X	X	X <sup>L</sup>	X	X			X	X <sup>L</sup>	O	O	T	Upper Kaponig Tal.
GD 208E		X				X	X	X		X	X		O		Upper Kaponig Tal.
GD 208F		X				X	X		O	X	X		O	AR	Upper Kaponig Tal.
GD 209A		{ O	X	X	O <sup>L</sup>	O		X		O	X <sup>L</sup>				Upper Kaponig Tal.
		{ X <sup>2</sup>	X	X	X <sup>L</sup>	X	X	X			X <sup>L</sup>		O	AR	Upper Kaponig Tal.
GD 209B		X <sup>2</sup>	X	X	X <sup>L</sup>	X	X			X	X <sup>L</sup>		O	T	Upper Kaponig Tal.
GD 404		X <sup>2</sup>	X	O <sup>S</sup>		X <sup>2</sup>	X <sup>2</sup>			X			O	Z	Upper Rieken Graben.
GD 447		X <sup>2</sup>	X		X <sup>L</sup>	X	X				O <sup>L</sup>		O	A	Untere Hochalm See.
GD 451		X			X <sup>L</sup>	X	X		O	X	X		O	A	Obere Hochalm See.
GD 465B		{ X	X		X <sup>L</sup>	X	X		O	X			O		Upper Gössgraben.
		{ O	X	O	O <sup>L</sup>	O	X	X					O	A	
C523				X <sup>H</sup>	X	X	X			X	X <sup>L</sup>			R	Pfaffenberger Seen.
RN 245		X <sup>H</sup>				X <sup>H</sup>	X <sup>2</sup>		O		X				Obere Zwenberger See.
RN 246		X <sup>2</sup>	O	O <sup>S</sup>		X <sup>2</sup>	X <sup>2</sup>			X	X				Obere Zwenberger See.
RN 247		X <sup>2</sup>		O <sup>S</sup>		X <sup>2</sup>	X <sup>2</sup>			X	X				Obere Zwenberger See.



Table 2 Mineral assemblages of representative Peripheral Schieferhülle metapelites. Explanation as for Table 1. G: Graphite. Superscript: i: present only as inclusions in garnet.

	GT	ST	KY	CTD	CHL	BIOT	MUSC	PAR	EP	QZ	PLAG	MT	ILM	ACC	LOCALITY	
GARNET + CHLORITE ZONE																
GD 36A	X				O	X	X			X	X <sup>L</sup>		O	G	Lower Zwenberger Tal road.	
GD 155	X				X	X	X			X	X <sup>L</sup>		O	TG	Lower Kaponig Tal road.	
GD 234C	O			X	X		X			X		X	X		Mühdorfer Graben road.	
GD 492	X				X	O	X		O	X					Oswald Hütte, Mallnitz.	
GD 498A				X	X		X		O	X		X	O		Oswald Hütte, Mallnitz.	
GD 561	X				X		X			X	X <sup>L</sup>		O	T	Törl Kopf-Rissieck ridge.	
GD 572B	X			X	X		X			X			O	TA	Jamnic Alm road, Tauern Tal.	
GD 771				X	X		X			X			O	T	Laschgwand, Tauern Tal.	
GD 789				X	X		X		O	X			O	A	N. side Tauern Tal.	
GD 792A	X			X	X		X			X			O		N. side Tauern Tal.	
GD 947B	X			X	X		X		O	X		X		A	Upper Tauern Bach.	
GARNET + STAUROLITE + CHLORITE SUBZONE																
GD 28B	X				X		X		O	X	X <sup>L</sup>	X		A	Lower Zwenberger Tal road.	
GD 43	X				X	X	X		X	X	X	O		T	Lower Zwenberger Tal road.	
GD 43B	X	X		X	X		X		O	X	X <sup>L</sup>	O	O	A	Lower Zwenberger Tal road.	
GD 308C	O	X		X	X		X		O	X		O		TA	Gatterinig Alm, Penk.	
GD 309C		X		X	O		X			X		O		A	Gatterinig Alm, Penk.	
GD 310B	X			O	X		X		O	X		O	O	TA	Gatterinig Alm, Penk.	
CHLORITOID + BIOTITE ZONE																
GD 168A				X		X	X	O	O	X			O	A	Labiges Köpfl.	
GD 168B	X			X	O	X	X		O	X			O	TA	Labiges Köpfl.	
GD 280B	O			X	X	X	X		O	X	O <sup>L</sup>		O	T	Sicker Kopf.	
GD 304	X			X	O	X	X			X			O	A	Sicker Kopf.	
GD 1289B				X		X	X		O	X			O	TA	N. side Törl Kopf, Mallnitz.	
GD 1289D	X			X	O	X	X			X			O	TA	N. side Törl Kopf, Mallnitz.	
STAUROLITE + BIOTITE ZONE																
GD 15B	X	O			O	X	X		O	X		O	O	TA	Lower Zwenberger Tal road.	
GD 18	X	X	X	O <sup>i</sup>	O	X	X	X	O	X	X <sup>L</sup>		O	A	Lower Zwenberger Tal road.	
GD 49C	X				O	X	X		X	X	X <sup>L</sup>			G	Lower Zwenberger Bach.	
GD 50B	X	O	O	O <sup>i</sup>		X	X		O	X	X <sup>L</sup>		O	TAR	Lower Zwenberger Bach.	
GD 50C	X	X		O <sup>i</sup>	O	X	X		O	X			O	TA	Lower Zwenberger Bach.	
GD 189	X	X			X	X	X			X	X <sup>2</sup>		O	AG	Zwenig Alm, Kaponig Tal.	
GD 202B	X	O		O <sup>i</sup>	X	X	X		O	X	X		O	O	A	W. side Gröneck.
GD 296	X	X		X		X	X			X			O	T	Sicker Kopf.	
GD 348	X	X		X	X	X	X			X	X		O	TA	Labiges Köpfl.	
GD 365	O	O				X	X		O	X	X <sup>2</sup>		O	TAG	Leutschacher Alm, Gröneck.	
GD 438	X	X	X		O	X	X		O	X	X <sup>L</sup>		O	TA	Lower Rieken Bach.	
GD 1296	X <sup>2</sup>	X		X	X	X	X			X			O	TA	Quatschnig, Dösender Tal.	
GD 1297B	X	X		X	O	O	X			O			O	TA	Quatschnig, Dösender Tal.	
GD 1297D	X	X		X	X	X	X			X			O	T	Quatschnig, Dösender Tal.	

The distinction between Alpine and pre-Alpine minerals is based partly on a study of the textural relationships (as seen in thin section) between mineral grains and micro-fabric elements such as schistosity or crenulations, and partly on the field distinction between fabrics which deform Zentralgneis aplites (possibly Alpine) and those which are cut by aplites (definitely pre-Alpine). If a particular microstructure can be ascribed to one of a sequence of recognised phases of deformation, one can then correlate phases of mineral growth in widely spaced rocks and arrange the different growth phases in a crude relative time sequence. This method has been successfully applied to other regional metamorphic terrains, e.g. the Scottish Caledonides (HARTE and JOHNSON, 1969) and

the Pyrenees (ZWART, 1963). A detailed account of the use of mineral textures in the understanding of the pre-Alpine and Alpine metamorphic history of the eastern Tauern will be presented separately, but a summary of the findings relevant to metapelites is given in fig. 5. The main conclusions are as follows:

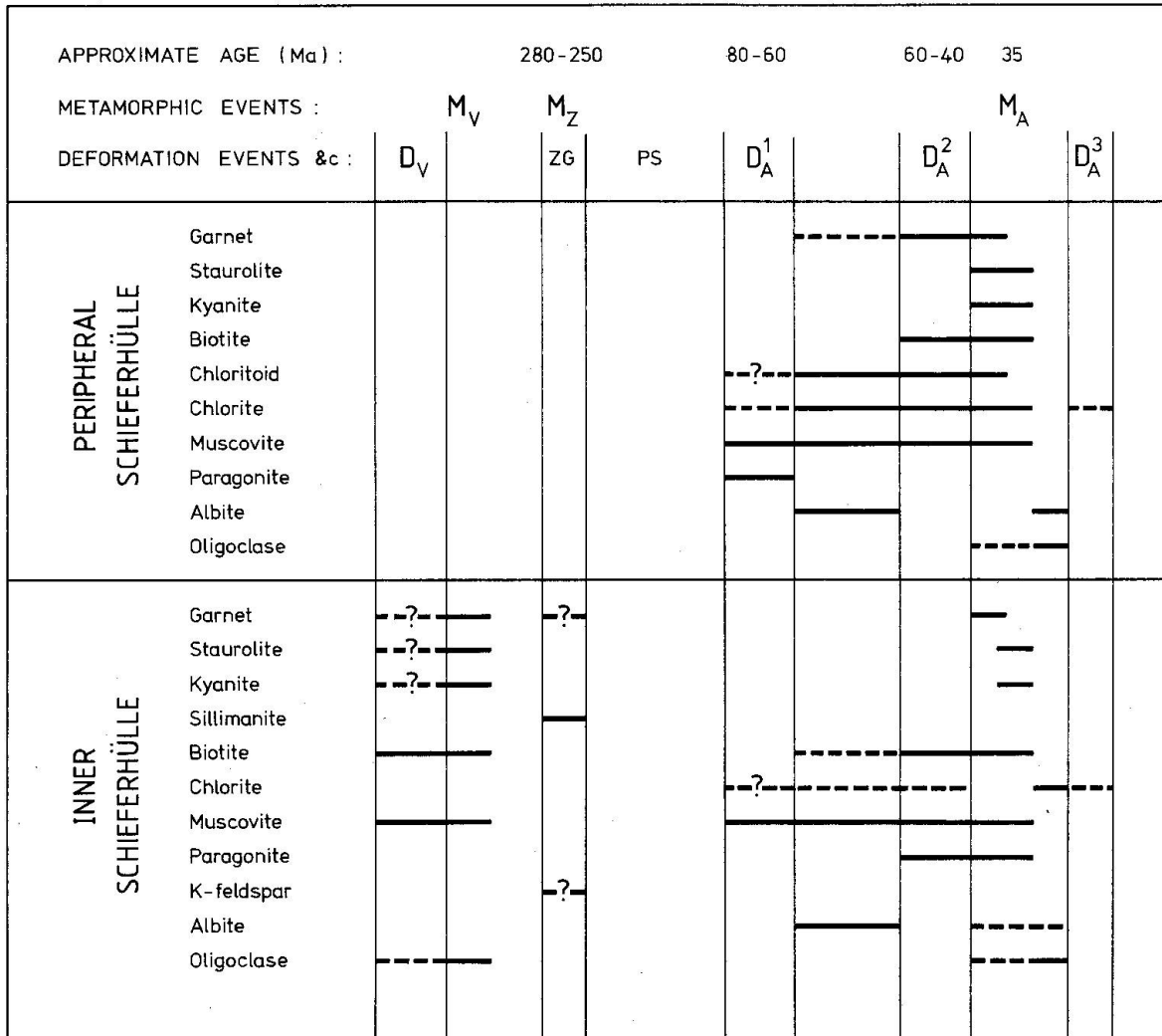


Fig. 5 Time relations of mineral growth in metapelites of the south-east Tauern Window. ZG: intrusion of Zentralgneis, PS: deposition of Peripheral Schieferhülle.

(i) The rounded cores of the large garnet porphyroblasts of Inner Schieferhülle metapelites are pre-Alpine, as are the strained muscovite porphyroblasts and rare bent staurolites and kyanites. Some biotites are probably also pre-Alpine. These minerals probably crystallised in a Hercynian amphibolite-facies regional metamorphism. Some of the pre-Alpine muscovites contain kyanite pseudomorphs after an acicular mineral, probably sillimanite (fig. 3 f), which is

thought to have grown as the result of partial thermal decomposition of muscovite during the intrusion of the Zentralgneis.

(ii) The «pin-prick» garnets and the bulk of the staurolite and kyanite in the Inner Schieferhülle are Alpine. These minerals crystallised after the second Alpine phase of penetrative deformation ( $D_a^2$ ). Since no minerals indicative of higher temperatures occur, the growth of staurolite and kyanite marks the Alpine metamorphic temperature peak.

(iii) Maximum temperature mineral assemblages in the Peripheral Schieferhülle metapelites also crystallised after  $D_a^2$ , although in the low-grade area west of Mallnitz occurrences of post- $D_a^2$  ferromagnesian silicates are rare, and the majority of peak temperature assemblages appear to have developed during  $D_a^2$ .

### Chemical mineralogy

Major element compositions of Alpine metapelite minerals were measured on a Cambridge Instruments Microscan-9 electron microprobe. Specimen preparation techniques are similar to those described by SWEATMAN and LONG (1969). Analyses are performed at 20 kV with a specimen current of  $2 \times 10^{-8}$  amps, and subsequently processed using the M-9 ZAF correction program.

Representative analyses of AFM minerals are listed in table 3.

(i) *Garnet*: All analysed garnets from the SE Tauern metapelites are zoned, but zoning profiles and garnet compositions are extremely varied making it difficult to generalise. Some examples are shown in figs. 6 and 7.

Inner Schieferhülle metapelite garnets with optically distinct pre-Alpine cores and Alpine rims have marked discontinuities in their zoning profiles at the core-rim boundaries (fig. 6 A and C), confirming that the cores and rims grew under different metamorphic conditions. Profile A (fig. 6) is a spectacular example. In this garnet, the core and rim have compositions so different that the sharp core-rim interface gives a Becke line. Ca shows the greatest variation, with rim concentrations being about ten times those in the core. The host rock in this case (GD1197) is a low-alumina albite rich schist from an area of comparatively low Alpine metamorphic grade. The difference in Ca concentration between core and rim could be explained if the cores equilibrated with calcic plagioclase in a comparatively hot Hercynian metamorphism. In the absence of epidote, the Ca released by the conversion of plagioclase to albite in Alpine times would have to reside in the garnet rims. «Pin-prick» garnets from this rock have compositions similar to the porphyroblast rims (fig. 6, profile B).

Garnets from Peripheral Schieferhülle metapelites tend to have smooth zoning profiles (fig. 7 and CLIFF et al., 1971, p. 173). In the rare cases where two size populations of garnet occur in one rock (fig. 7, profiles C and D) both types

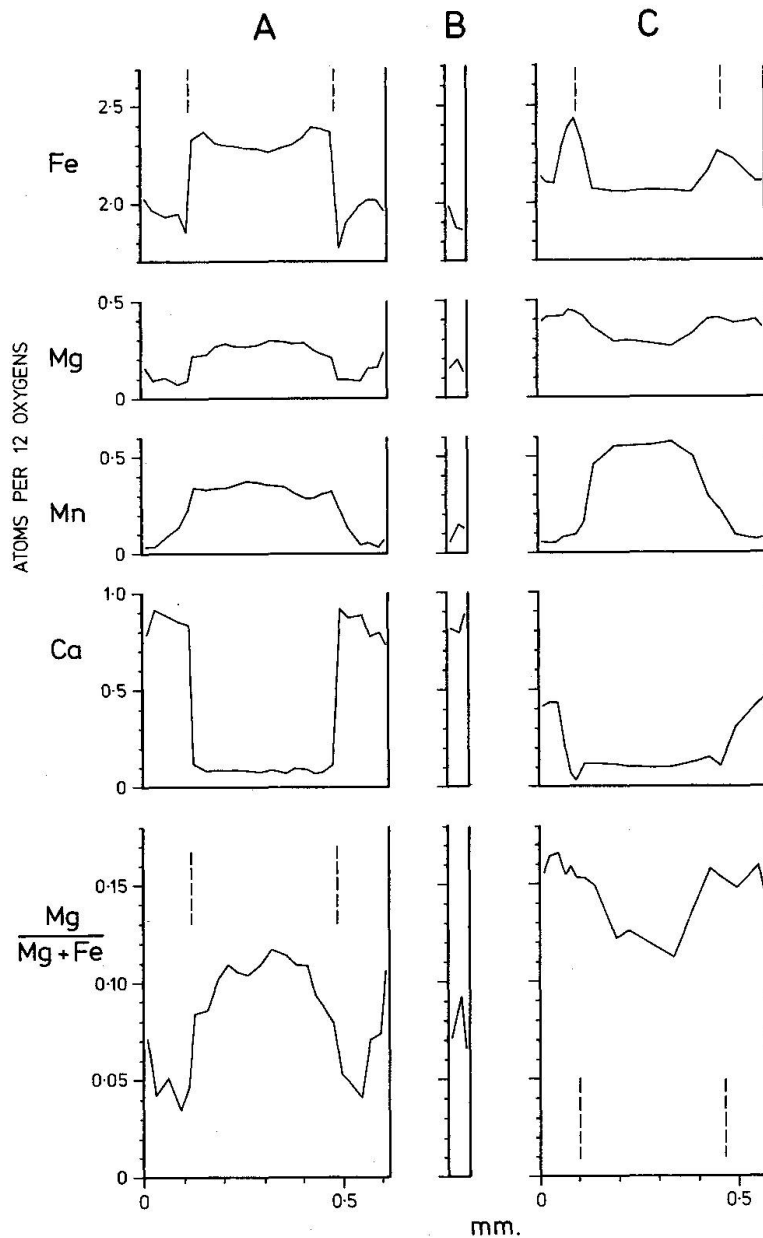


Fig. 6 Garnet zoning profiles from Inner Schieferhülle metapelites.  
 A. Large optically zoned garnet. GD1197. 25 analyses.  
 B. Small euhedral garnet. GD1197. 3 analyses.  
 C. Large optically zoned garnet. GD447. 18 analyses.  
 Dashed lines mark position of core-rim interface.

show identical zonation trends, but the core compositions of the smaller crystals correspond to the near-rim compositions of the porphyroblasts, while the rim compositions of the two types are almost identical. In the pair illustrated in fig. 7, garnet D appears to have nucleated when garnet C had grown to about 0.8 of its present diameter. In all analysed Peripheral Schieferhülle garnets, Mg and  $\text{Mg}/\text{Mg} + \text{Fe}^{2+}$  increase from core to rim, suggesting that the profiles formed as the result of garnet growth during increasing temperature conditions.

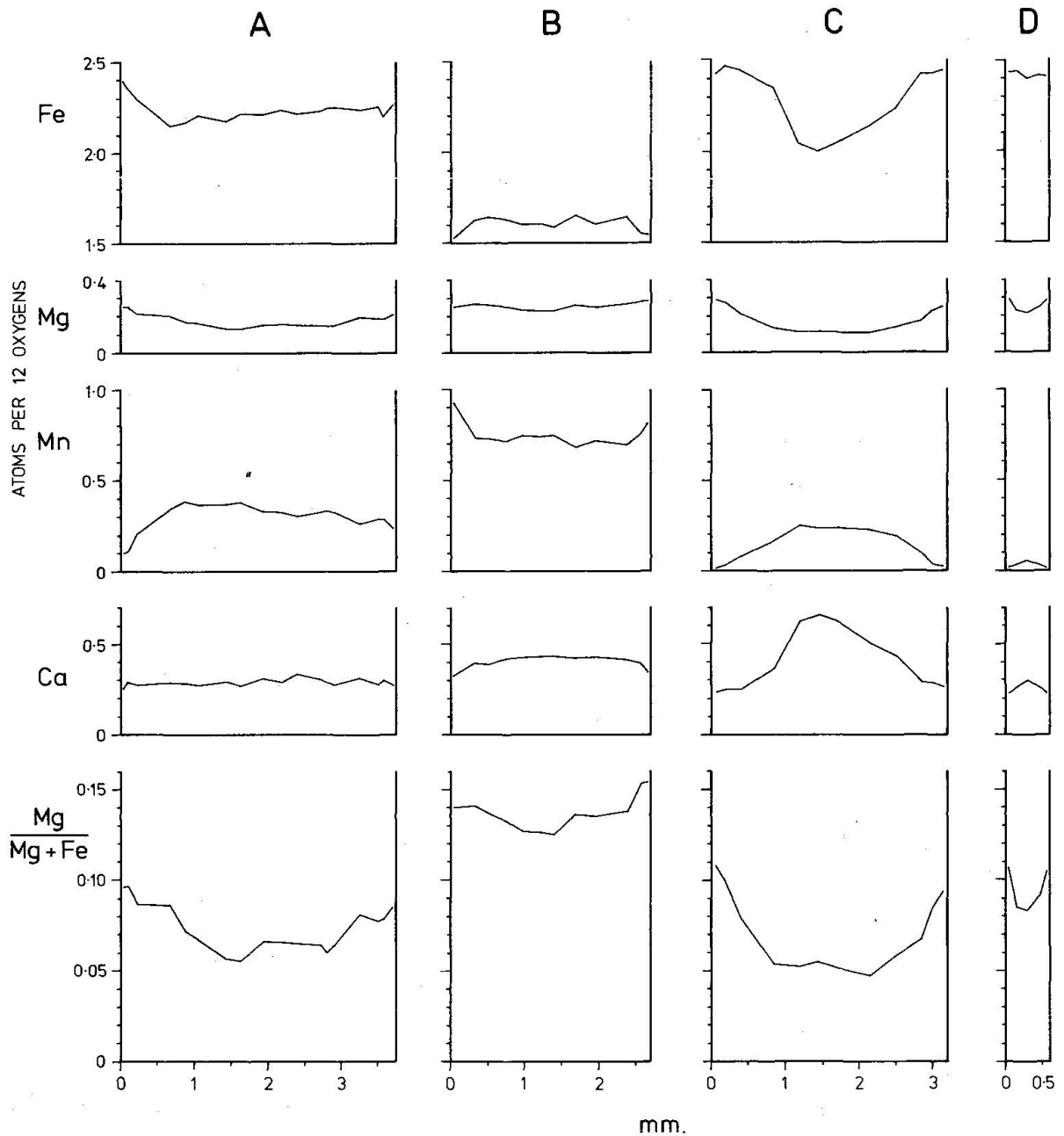


Fig. 7 Garnet zoning profiles from Peripheral Schieferhülle metapelites.  
 A. Subhedral post- $D_2^a$  garnet. GD 168 b. Traverse  $\perp$  schistosity. 17 analyses.  
 B. Flat post- $D_2^a$  garnet. GD 308 c. Traverse  $\parallel$  schistosity. 12 analyses.  
 C. Large rounded garnet porphyroblast. GD 1296. Traverse  $\perp$  schistosity. 12 analyses.  
 D. Small euhedral garnet. GD 1296. Traverse  $\parallel$  schistosity. 5 analyses.

Other elements, such as Mn, are less consistent. Some garnets (e.g. A, C, and D in fig. 7) display the normal trend of decreasing Mn from core to rim, while others (e.g. B in fig. 7) show the opposite. Possible reasons for this are discussed in the section headed "Reaction Textures".

(ii) *Chlorite*: Most analysed chlorites are magnesian ripidolites according to the classification of HEY (1954). Primary (i.e. non-retrogressive) syn- $D_2^a$  and

post- $D_a^2$  chlorites from the south-east Tauern resemble the majority of pelitic chlorites in that they plot close to the composition  $(Mg\ Fe)_9Al_6Si_5O_{20}(OH)_{16}$  (VELDE and RUMBLE, 1977).

(iii) *Biotite*: All analysed biotites contain significantly more Al than phlogopite or annite. This is largely due to  $Al^{vi}Al^{iv} = (Mg\ Fe)^{vi}Si^{iv}$  substitution (RUTHERFORD, 1973), but the fact that the ratio  $Si/Mg + Fe + Mn$  is always greater than unity suggests some  $2Al^{iv} = 3(Mg\ Fe)^{iv}$  substitution, i. e. towards phengitic dioctahedral micas.  $Mg/Mg + Fe$  ratios fall close to 0.5 in most analysed metapelitic biotites.

(iv) *Chloritoid*:  $Mg/Mg + Fe$  ratios of chloritoids range from 0.13 to 0.25. Appreciable Mn concentrations occur in some chloritoids (e.g. over 5% Mn endmember in GD308c). No significant zoning was detected in large pre- $D_a^2$  porphyroblasts.

(v) *Staurolite*: Staurolite analyses have been recalculated to 47 oxygens in accordance with the idealised composition  $(Fe\ Mg)_4(Al\ Fe)_{18}Si_8O_{46}(OH)_2$  proposed by NARÁY-SZABÓ and SASVÁRI (1958). Cation totals and Si:Al stoichiometries agree tolerably well with this formula, though there are considerable variations in  $Fe + Mg + Mn$ . 0.09% ZnO was detected in staurolites in GD1296.  $Mg/Mg + Fe$  ratios range from 0.13 to 0.21. No concentric or sector zoning was detected.

(vi) *White-micas*: Most analysed metapelite muscovites contain between 10 and 25% celadonite solid solution. The lowest values are from aluminous Inner Schieferhülle schists. These rocks also contain the muscovites with the highest Na contents, with up to 30% paragonite solid solution in grains coexisting with a paragonite phase. The paragonites themselves contain up to 17% muscovite and 6% margarite components.

Many analysed white-micas are deficient in alkalis, with  $Na + K + Ca$  totalling between 1.7 and 1.9 atoms per 22 oxygens. This phenomenon is generally attributed to  $H_3O^+$  ions substituting for  $K^+$  and  $Na^+$  in the interlayer sites (BUTLER, 1967; CIPRIANI et al., 1971).

#### AFM-phase relations

Most metapelites in the area studied can be represented by the system  $FeO$ - $MgO$ - $Al_2O_3$ - $SiO_2$ - $K_2O$ - $H_2O$  (KFMASH) provided that certain assumptions are made:

(i) The abundant late porphyroblasts of plagioclase grew metasomatically at the expense of white mica after the peak of metamorphism, and need not be considered part of the peak metamorphic assemblage; i. e. the bulk of  $CaO$  and  $Na_2O$  were introduced at a late stage.

	GARNETS						BIOTITES			
	GD465b	GD168b	GD18	GD308c	GD1296	GD1296	GD465b	GD168	GD168b	GD18
	M	PR	PR	PC	PC	PR	M	M	M	M
SiO <sub>2</sub>	37.76	37.53	37.67	37.31	37.51	37.39	35.42	35.80	37.89	36.68
TiO <sub>2</sub>	0.21	0.07	0.07	0.14	0.00	0.00	1.62	1.34	1.55	1.47
Al <sub>2</sub> O <sub>3</sub>	21.04	20.83	20.57	20.58	21.11	20.11	19.00	19.16	17.53	18.54
Fe <sub>2</sub> O <sub>3</sub>	0.39	0.00	0.79	0.58	0.17	0.21	-	-	-	-
FeO	34.04	35.13	30.94	23.88	30.49	36.41	18.35	20.72	20.97	20.56
MnO	1.56	1.67	2.56	10.89	3.52	0.48	0.05	0.17	0.07	0.05
MgO	4.15	2.08	2.99	1.93	0.93	2.28	10.25	9.04	9.00	9.85
CaO	1.67	3.43	4.73	4.99	7.24	2.84	0.00	0.03	0.01	0.10
Na <sub>2</sub> O	0.00	0.00	0.00	0.00	0.00	0.00	0.19	0.33	0.29	0.36
K <sub>2</sub> O	0.00	0.00	0.00	0.00	0.00	0.00	9.35	8.40	8.60	8.47
TOT	100.82	100.74	100.32	100.30	100.97	100.41	95.23	94.99	95.91	96.08
Formula	12(O)						22(O)			
Si	3.00	3.01	3.00	3.00	3.00	3.01	5.50	5.46	5.71	5.52
Ti	0.01	0.00	0.00	0.01	0.00	0.00	0.18	0.15	0.18	0.17
Al	1.97	1.97	1.94	1.95	1.99	1.98	3.38	3.45	3.12	3.29
Fe <sup>III</sup>	0.02	0.00	0.05	0.04	0.01	0.01	-	-	-	-
Fe <sup>II</sup>	2.26	2.36	2.07	1.60	2.04	2.46	2.32	2.65	2.65	2.59
Mn	0.11	0.11	0.17	0.74	0.24	0.03	0.01	0.02	0.01	0.01
Mg	0.49	0.25	0.36	0.23	0.11	0.27	2.31	2.06	2.02	2.21
Ca	0.14	0.30	0.41	0.43	0.62	0.25	0.00	0.01	0.00	0.02
Na	0.00	0.00	0.00	0.00	0.00	0.00	0.06	0.10	0.09	0.11
K	0.00	0.00	0.00	0.00	0.00	0.00	1.80	1.64	1.65	1.63
TOT	8.00	8.00	8.00	8.00	8.01	8.01	15.56	15.54	15.53	15.55

Table 3 Microprobe analyses of AFM-minerals.

(ii) The minor components Fe<sub>2</sub>O<sub>3</sub> and TiO<sub>2</sub> and the original CaO and Na<sub>2</sub>O can be ignored because each is abundant in only one equilibrium mineral (magnetite, ilmenite, epidote and albite or paragonite, respectively). The Gibbs phase rule predicts that the equilibrium relations among other phases will not be affected if these components and the phases containing them are both excluded from consideration.

(iii) The component MnO can be ignored as it is not a saturating component in any phase. (THOMPSON et al., 1977 a).

The mineral parageneses in muscovite + quartz-bearing metapelites can therefore be treated using the AFM projection of THOMPSON (1957) provided that it is also assumed that (a) H<sub>2</sub>O behaved as a perfectly mobile component, and (b) one can legitimately project from muscovite (even though muscovite is not present as a pure phase) without altering the topology of the AFM diagram. Ignoring retrogressive chlorite and inclusions isolated from matrix minerals by enclosing porphyroblasts, the following AFM assemblages (+ excess components) can be distinguished:

			CHLORITES				CHLORITIDS						STAUROLITES			
	GD280b	GD1296	GD465b	GD308c	GD280b	GD1296	GD168	GD168b	GD308c	GD280b	GD1296	GD1296	GD465b	GD18	GD308c	GD1296
	M	M	PC	M	M	M	PR	PR	PR	M	I	M	PR	PR	M	PR
SiO <sub>2</sub>	36.49	36.85	24.35	25.23	24.42	24.35	24.17	24.30	24.83	24.25	24.11	24.33	28.10	27.93	28.33	28.04
TiO <sub>2</sub>	1.34	1.67	0.09	0.05	0.10	0.00	0.03	0.00	0.02	0.02	0.00	0.00	0.45	0.36	0.18	0.31
Al <sub>2</sub> O <sub>3</sub>	19.07	19.64	22.40	22.84	21.93	23.02	40.57	40.60	40.68	40.95	40.91	40.78	52.71	52.87	54.83	54.41
Fe <sub>2</sub> O <sub>3</sub>	-	-	-	-	-	-	0.59	0.76	1.80	0.39	0.00	0.16	-	-	-	-
FeO	19.57	18.98	23.35	20.07	25.77	24.98	23.81	23.48	20.82	23.18	24.85	22.86	14.18	14.34	11.26	12.83
MnO	0.07	0.00	0.09	0.55	0.16	0.00	0.85	0.17	1.51	0.47	0.34	0.00	0.09	0.24	0.85	0.00
MgO	9.71	9.44	15.81	18.12	13.92	14.31	2.30	2.87	3.88	2.98	1.72	3.08	1.93	1.54	1.61	0.96
CaO	0.03	0.09	0.01	0.01	0.06	0.00	0.00	0.00	0.00	0.00	0.00	0.00	0.00	0.01	0.01	0.00
Na <sub>2</sub> O	0.22	0.00	0.00	0.02	0.02	0.00	0.00	0.00	0.00	0.00	0.00	0.00	0.00	0.05	0.03	0.00
K <sub>2</sub> O	8.78	8.08	0.00	0.04	0.01	0.00	0.00	0.00	0.00	0.00	0.00	0.00	0.00	0.01	0.01	0.00
TOT	95.28	94.75	86.10	86.93	86.39	86.66	92.32	92.18	93.54	92.24	91.93	91.19	97.46	97.35	97.11	96.98*
Formula			28(0)				12(0)						47(0)			
Si	5.52	5.55	5.18	5.22	5.25	5.18	2.00	2.01	2.01	2.00	2.01	2.02	8.01	7.98	8.00	7.98
Ti	0.15	0.19	0.01	0.01	0.02	0.00	0.00	0.00	0.00	0.00	0.00	0.00	0.10	0.08	0.04	0.07
Al	3.40	3.49	5.62	5.57	5.56	5.78	3.96	3.95	3.89	3.98	4.01	3.99	17.71	17.81	18.25	18.25
Fe <sup>III</sup>	-	-	-	-	-	-	0.04	0.05	0.11	0.02	0.00	0.01	-	-	-	-
Fe <sup>II</sup>	2.48	2.39	4.15	3.48	4.63	4.44	1.65	1.62	1.40	1.60	1.73	1.68	3.38	3.43	2.66	3.05
Mn	0.01	0.00	0.02	0.10	0.03	0.00	0.06	0.01	0.11	0.03	0.02	0.00	0.02	0.06	0.20	0.00
Mg	2.19	2.12	5.01	5.59	4.46	4.54	0.28	0.35	0.47	0.37	0.22	0.38	0.82	0.66	0.68	0.41
Ca	0.01	0.02	0.00	0.00	0.01	0.00	0.00	0.00	0.00	0.00	0.00	0.00	0.00	0.00	0.00	0.00
Na	0.07	0.00	0.00	0.01	0.01	0.00	0.00	0.00	0.00	0.00	0.00	0.00	0.00	0.03	0.02	0.00
K	1.69	1.55	0.00	0.01	0.00	0.00	0.00	0.00	0.00	0.00	0.00	0.00	0.00	0.00	0.00	0.00
TOT	15.52	15.31	19.99	19.99	19.97	19.94	7.99	7.99	7.99	8.00	7.99	7.98	30.04	30.05	29.85	29.85*

\*Includes 0.09% ZnO

M: small grain in matrix, PC: porphyroblast core, PR: porphyroblast rim, I: inclusion in garnet core.

- |                        |                                |
|------------------------|--------------------------------|
| 1. gt + chl            | 9. gt + ctd + biot + chl       |
| 2. gt + biot + chl     | 10. ctd + biot + chl           |
| 3. gt + ctd + chl      | 11. gt + st + ctd + biot       |
| 4. ctd + chl           | 12. gt + st + ctd + biot + chl |
| 5. st + ctd + chl      | 13. gt + st + biot             |
| 6. gt + st + ctd + chl | 14. gt + st + biot + chl       |
| 7. ctd + biot          | 15. gt + st + ky + biot        |
| 8. gt + ctd + biot     | 16. gt + st + ky + biot + chl  |

In most of these assemblages, the chemographic relationships are the same, with Mg/Mg + Fe ratios increasing in the order garnet < staurolite < chloritoid < biotite < chlorite. This is identical to the sequence found by ALBEE (1972) and RUMBLE (1974) in pelites from many different localities. In some rocks with assemblages 15 and 16, garnet rims have virtually identical Mg/Mg + Fe ratios as coexisting staurolites.



Compatibility relationships between the assemblages with three AFM phases or less (i.e. nominal variance of two or more) are shown schematically in fig. 8. Three groups of compatible high-variance AFM assemblages can be distinguished: (a) 1, 2, 3, 4, 5; (b) 4, 5, 7, 8, 10; (c) 13. Crossed tie-line relationships exist between these groups (fig. 8) and form the basis of delineating the metamorphic zones described in the following section.

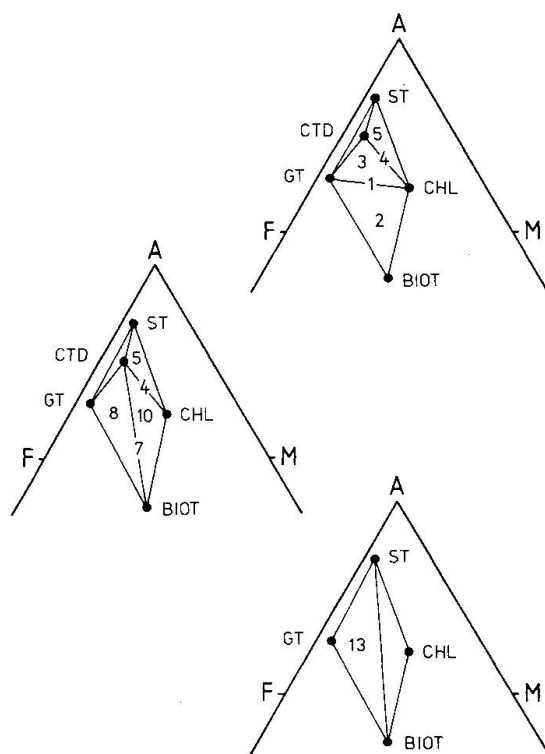


Fig. 8 Schematic THOMPSON (1957) AFM-projections showing the compatibility relationships among AFM-mineral assemblages with nominal variance greater than one. Numbers refer to assemblages listed in the text.

Several explanations could account for the low variance assemblages 6, 9, 11, 12, 14, 15 and 16. They could be:

(i) truly univariant or invariant equilibrium assemblages collected from discontinuous reaction isograds: – In view of the vanishingly small probability of sampling a univariant line or invariant point, it is extremely unlikely that this explanation can account for many of the numerous occurrences of overdefined assemblages.

(ii) Divariant equilibrium assemblages in which an «AFM» phase is saturated with respect to a component hitherto ignored in this system, such as Ca or Mn in garnet (e.g. HOUNSLOW and MOORE, 1967): – were this the case, one would expect the distribution of low variance assemblages to be purely a function of rock composition and hence essentially random in the area studied. The

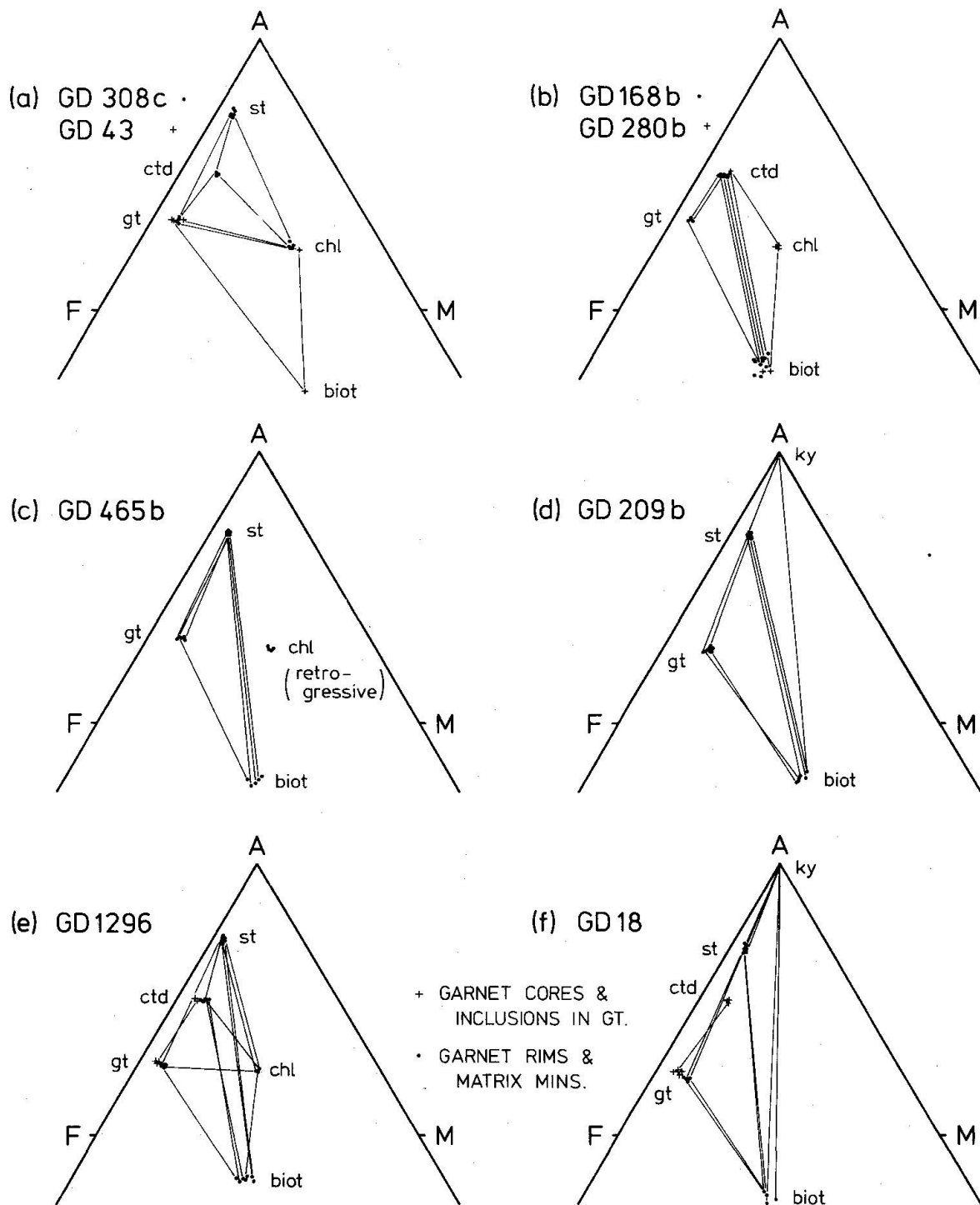


Fig. 9 THOMPSON (1957) AFM-projection for 8 metapelites. (a) gt + st + chl subzone; (b) ctd + biot zone; (c)–(f) st + biot zone.

fact that these assemblages are concentrated in the high-grade part of the area, and that, with one exception (GD308c), the garnets of four- and five-phase assemblages do not contain appreciably higher Ca and Mn contents than those of three-phase assemblages, suggests that this explanation is incorrect.

(iii) Divariant equilibrium assemblages in which a non-saturating component (e.g. Mn) is present in sufficient concentration to cause a discontinuous (Fe, Mg) reaction to become a continuous (Fe, Mg, Mn) reaction (e.g. THOMPSON et al., 1977 [b]): – this explanation is supported by the existence of appreciable concentrations of Ca in garnet and of Mn in chloritoid, staurolite and garnet in many analysed rocks.

(iv) Equilibrium reacting assemblages which buffered  $a_{\text{H}_2\text{O}}$  in the fluid phase (e.g. EVANS and GUIDOTTI, 1965; MELSON, 1966; TROMMSDORFF, 1968, 1972; GREENWOOD, 1975): – In this case the assumption that  $\mu_{\text{H}_2\text{O}}$  was externally controlled is wrong and use of the AFM projection is invalid.

(v) Disequilibrium assemblages in which the non-reactive nature of a mineral (e.g. garnet) prevented it from being exhausted in the course of a reaction when it would have been had equilibrium been achieved on the scale of a thin-section (e.g. HOLLISTER, 1969; ATHERTON and BROTHERTON, 1972): – this is likely to result in the development of mm-scale domains with different bulk compositions and containing different, but compatible three-phase assemblages. Many of the "low variance" metapelites show this feature, but in a few, incompatible three-phase assemblages are found interspersed on a millimetre scale (e.g. st + ctd + chl, st + biot + chl, st + ctd + biot, ctd + biot + chl, gt + st + biot and gt + st + ctd in GD 1296).

The association of overdefined assemblages with the closely spaced isograds (fig. 10) and the presence, in some rocks, of reaction textures (p. 261–265) support explanations (iii), (iv) and (v) at the expense of (i) and (ii).

AFM projections for some of the analysed rocks are shown in fig. 9.

### Metamorphic zones and isograds

Three distinct metamorphic zones can be mapped in quartz-bearing pelitic schists (fig. 10): –

(i) Garnet + chlorite zone (lowest grade – assemblages 1 to 4) covering the area west of Mallnitz and the south-western part of the Mölltal Schieferhülle.

(ii) Staurolite + biotite zone (highest grade – assemblages 11 to 16) covering the structurally lowest part of the Mölltal Schieferhülle and basement of the Hochalm Kern.

(iii) Chloritoid + biotite zone (intermediate grade – assemblages 7 to 10) occupying a thin 100–200 m wide area between (i) and (ii) but apparently wedging out towards the south-east.

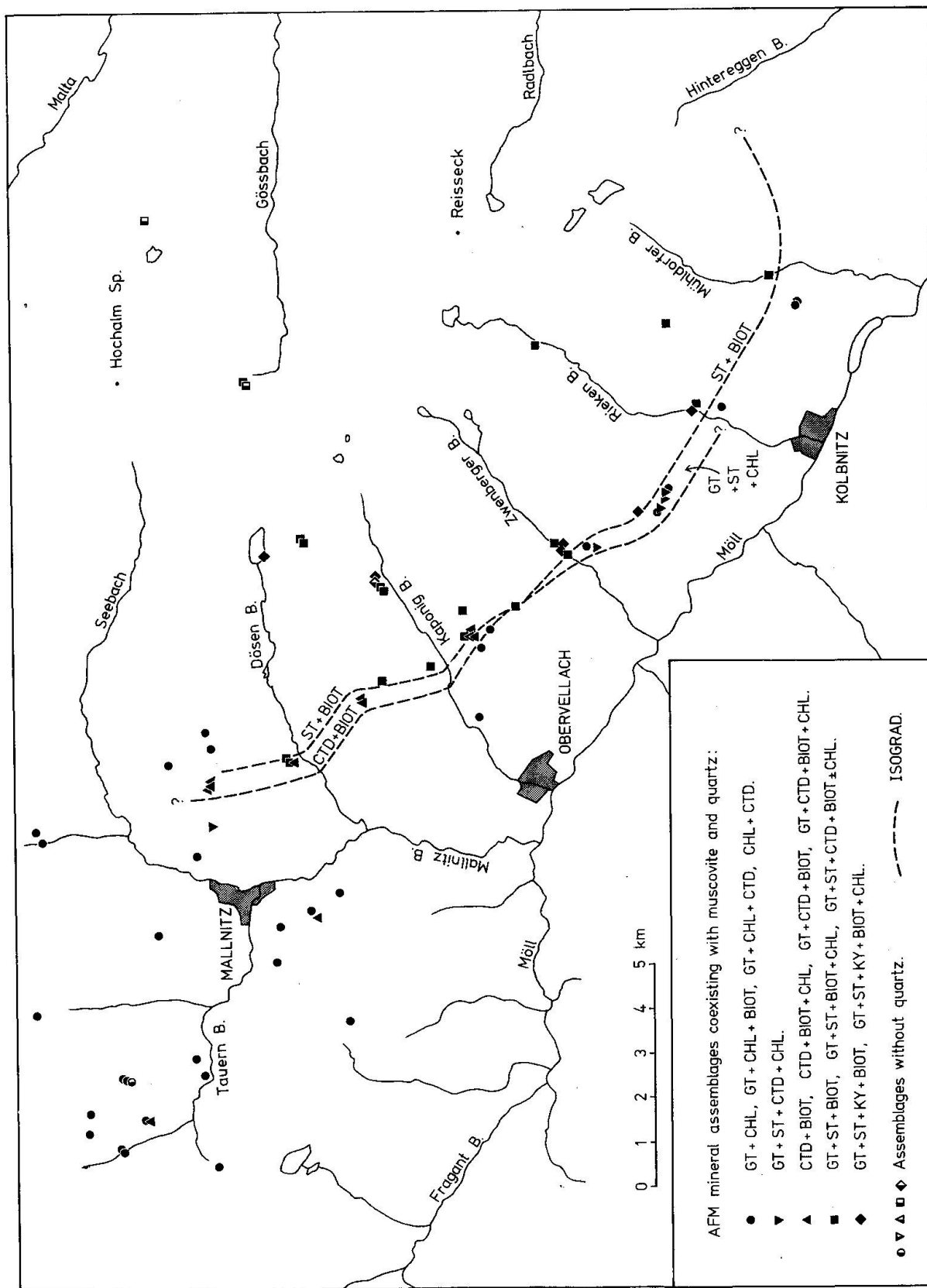


Fig. 10 The distribution of Alpine AFM-mineral assemblages in the south-east Tauern Window.

In addition, an ill-defined area characterised by assemblage 6, the garnet + staurolite + chlorite subzone, occurs in the highest grade part of the garnet + chlorite zone, but only where the chloritoid + biotite zone is absent.

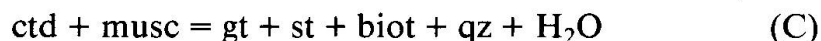
These metamorphic zones are bounded by isograds which mark the first appearance of the defining assemblage proceeding up grade. Overdefined assemblages are included on the high-grade side of the appropriate isograd (e.g. assemblage 9 is placed in the chloritoid + biotite zone, not the garnet + chlorite zone). The isograds can be modelled on the following discontinuous reactions:



(chloritoid + biotite isograd)



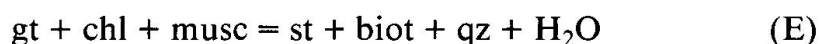
(staurolite + biotite isograd north of Obervellach)



(not mappable as an isograd)



(garnet + staurolite + chlorite isograd)



(staurolite + biotite isograd south of Obervellach)

The isograds are thus true isograds in the sense of CARMICHAEL (1970) and FREY (1974) in that they represent discontinuous reactions, and not merely the first appearance of certain index minerals proceeding up-grade, as in TILLEY (1924). Reactions A and B correspond to the crossed tie-line relationships illustrated in fig. 8.

The relationship between the univariant reactions A to E and the associated divariant assemblages can be represented by a Schreinemaker's bundle (ZEN, 1966) in which they are arranged in P-T-space around an invariant point  $\text{gt} + \text{st} + \text{ctd} + \text{chl} + \text{biot} + \text{musc} + \text{qz}$  (fig. 11). The temperature axis can be orientated knowing that  $\text{H}_2\text{O}$  is evolved on the high temperature side of each equilibrium, and that staurolite is stable at higher temperatures than chloritoid, as shown experimentally by HALFERDAHL (1961), HOSCHEK (1967, 1969), GANGULY (1968), GANGULY and NEWTON (1968) and RICHARDSON (1968). The orientation of the pressure axis is less obvious and is discussed on p. 266. The arrangement of isograds on the ground surface is entirely consistent with this topology, in particular the apparent mutual exclusion of the chloritoid + biotite zone and garnet + staurolite + chlorite subzone.

The scarcity of pelitic units in the Mölltal Schieferhülle makes it impossible to locate the isograds exactly, except in rare cases. The isograds are constrained well enough to show that they dip roughly parallel to the steep, south-west dipping  $D_2^a$  schistosity, but not well enough to show whether more or less steeply.

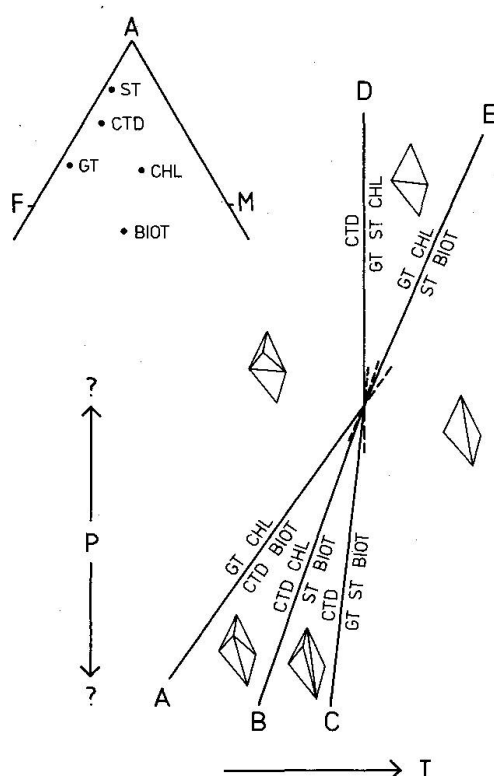


Fig. 11 Schematic Schreinemaker's P-T-net relating the univariant reactions involving garnet, staurolite, chori-toid, biotite, chlorite, muscovite, quartz and  $H_2O$  in the system KFMASH.

Late ( $D_3$ ) updoming, centred on the Hochalm Kern, seems to have rotated the isograds as well as the schistosity into a subvertical position. No discontinuity in metamorphic grade can be detected at the basement-cover interface.

The two isolated ctd + biot occurrences south and west of Mallnitz (fig. 10) have been ignored in the construction of isograds. Both rocks were collected within 5 m of thick marble units and may have equilibrated with fluids uncharacteristically rich in  $CO_2$ . However, it is unlikely that the bulk of the ctd + biot zone was stabilised in this way because the ctd + biot- and gt + st + chl-schists are found along strike from one another in similar geological settings.

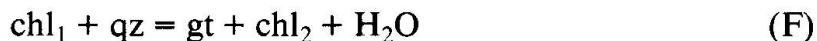
#### Reaction textures

In an overthrust such as the Pennine Zone of the Tauern Window, the "metamorphic geotherm" (or locus of P-T-points connecting the peak metamorphic conditions preserved in a sequence of exposed rocks) is likely to differ greatly from the actual P-T-path followed by any one rock in its metamorphic history (ENGLAND and RICHARDSON, 1977). Consequently, the model reactions discussed above may not, in fact, have occurred. The only sure way of identifying the actual reactions experienced by a given rock is by interpreting reaction tex-

tures and examining the relicts of earlier stages, such as core compositions and inclusion assemblages within zoned garnets (e.g. TRACY et al., 1976; THOMPSON et al., 1977 [b]). One major drawback of this approach is that earlier assemblages are always incomplete.

**(a) Garnet-forming reactions:**

Since garnet is present even in the lowest-grade metapelites of the south-east Tauern, garnet-forming reactions cannot be studied with reference to an isograd. Mineral textures are consistent with the generalised continuous reaction:



where  $\text{chl}_2$  has a higher Mg/Mg + Fe ratio than  $\text{chl}_1$ , and possibly a different Al/Mg + Fe ratio. The growth of garnet in schists containing neither biotite nor chloritoid suggests that these minerals need not participate. In many  $\text{gt} + \text{ctd} + \text{chl}$ -schists, the garnets have clearly grown at the expense of chlorite, but have overgrown chloritoids without apparently consuming them. As a result, chloritoid inclusions are common whereas chlorite inclusions are rare. The gradual increase in Mg/Mg + Fe<sup>2+</sup> ratio from core to rim in post-D<sub>a</sub><sup>2</sup> garnets (fig. 7) is also consistent with reaction F.

**(b) Intermediate-grade reactions; Kolbnitz area:**

In this sector, the first discontinuous reaction encountered involves only schists containing chloritoid (i.e. low grade assemblages 3 and 4). There is good textural evidence for the breakdown of chloritoid according to reaction D. Tiny euhedral prisms of staurolite and sprays for chlorite nucleate in and around chloritoid laths (fig. 4b). The formation of prograde chlorite at this stage is noteworthy. Taken on its own, this texture suggests the continuous reaction:



The association of magnetite with the product phases (fig. 4b) suggests that chloritoid breakdown via the oxidation reaction:



may have been important.

The effect of reaction G would be to move the three phase triangle  $\text{st} + \text{ctd} + \text{chl}$  towards more iron-rich compositions (THOMPSON, 1977) so that aluminous and magnesian  $\text{ctd} + \text{chl}$ -schists would gain staurolite as an extra phase without the involvement of garnet. However, all but one  $\text{st} + \text{ctd} + \text{chl}$ -schists found contain additional garnet. In GD43b, the original (pre-staurolite) AFM assem-

blage was  $gt + ctd + chl$ . Fig. 4a shows part of this rock where chloritoid, partially enclosed by garnet, has been incompletely replaced by staurolite and chlorite. As garnet was present long before chloritoid breakdown, discontinuous terminal reaction D must have been responsible, not reaction G. In other schists with assemblage 6, it is not clear whether the garnets grew before or during chloritoid breakdown as they have not nucleated at chloritoid grains. However, breakdown of the comparatively Mn-rich chloritoid in GD308c (table 2) after garnet growth could account for the unusual Mn-enrichment of garnet rims (fig. 7B) either (a) by accretion of an Mn-rich rim onto a pre-existing core or (b) by diffusion of the released Mn into a pre-existing garnet. Some Mn-rich garnet rims from other terrains are thought to have formed as the result of retrograde garnet resorption involving selective removal of Fe, Mg and Ca from garnet rims (e.g. GRANT and WEIBLEN, 1971; DALLMEYER, 1974 and DE BETHUNE et al., 1975). This explanation could not apply to GD308c because the garnets cut cleanly across a fine-grained schistose mica fabric and show no textural evidence of resorption.

Gt + chl  $\pm$  biot schists persist into the gt + st + chl subzone, being unaffected by reactions D, G and H. No rocks were found containing the biotite-free critical subzone assemblage gt + st + chl in which reaction D had gone to completion.

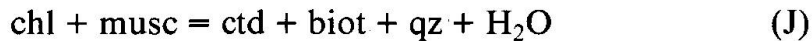
In staurolite + biotite schists from the Kolbnitz sector (e.g. GD50c), chloritoid has entirely disappeared from the matrix of the rocks but is still preserved locally as inclusions within garnet porphyroblasts. Biotite is more abundant than in metapelites of lower grade, chlorite less so. Euhedral staurolite prisms are closely associated with biotite and cluster round the perimeters of garnet grains in some rocks (as in fig. 4d). Together, these features suggest growth of staurolite and biotite at the expense of garnet and chlorite, presumably by reaction E.

(c) Intermediate-grade reactions; Mallnitz - Obervellach area: -

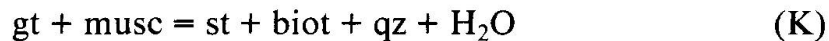
Schists of the ctd + biot zone provide good textural evidence for late growth of chloritoid and biotite. Both minerals commonly occur as random flakes cutting across a  $D_a^2$  schistosity. In rocks of this zone chloritoid and biotite are very commonly found in mutual contact, and there is little doubt that they represent an equilibrium assemblage (fig. 4c). Primary chlorite, on the other hand, rarely forms cross-cutting flakes in this zone, and is generally subordinate to garnet, chloritoid and biotite in rocks with assemblage 9, suggesting that much of it was consumed by reaction A. There is, however, no textural or chemical evidence to suggest that garnets were resorbed during this reaction. The occurrence, albeit rare, of the two-phase assemblage ctd + biot is significant in this respect, because it implies that if reaction A *did* occur, garnets must have been present at



an early stage and then totally consumed. The complete absence of possible pseudomorphs after garnet in schists with assemblage 7 suggests that this explanation is wrong. The most likely way of producing the assemblage ctd + biot in the absence of garnet is by the continuous (Fe Mg) reaction:



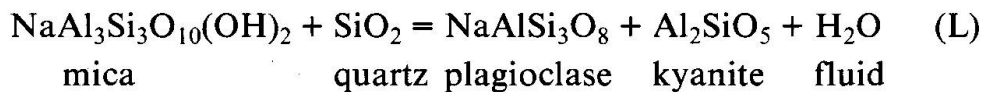
Since no highly aluminous schists have been found in the N.W. Mölltal Schieferhülle, the first recorded appearance of staurolite in this sector is at the staurolite + biotite isograd. In the few st + biot schists collected immediately upgrade of the ctd + biot zone, garnet, chloritoid and biotite persist, usually with chlorite, giving rise to assemblages 11 and 12. These over-defined rocks are generally devoid of clear-cut reaction textures, but one (GD1296) contains large garnet porphyroblasts locally rimmed by staurolite (fig. 4d). This texture cannot be explained by any of reactions A, B and C, but implies either discontinuous reaction E, or the continuous reaction:



(d) High-grade reactions:

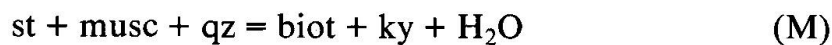
Staurolite + biotite assemblages persist to the structurally lowest parts of the basement. Kyanite is present as an additional phase in many schists of this zone (assemblages 15 and 16), but its occurrence is sporadic, and there is no evidence of a distinct kyanite zone as in the Scottish Highlands (BARROW, 1912; TILLEY, 1925; ATHERTON, 1977). Almost all recorded Alpine kyanite-schists from the south-east Tauern also contain staurolite, garnet and biotite.

Some of the kyanite-schists contain paragonite, so it is possible that kyanite was produced by the reaction:



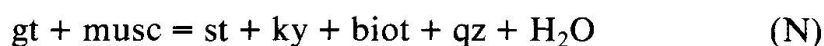
However, the importance of this reaction is doubtful because all the plagioclase in aluminous pelites appears to have grown after staurolite and kyanite crystallisation was complete (fig. 3d).

The breakdown of staurolite is commonly invoked to explain the first appearance of kyanite in metapelites. For example, CHINNER (1965) has shown that the kyanite isograd in the Scottish Dalradian reflects the continuous reaction:



In the south-east Tauern Window, however, there is no evidence for kyanite growth at the expense of staurolite, although some textures could be interpreted

as such, e. g. (i) the close association of kyanite and staurolite in rims round garnet porphyroblasts in Peripheral Schieferhülle schists GD 18 and GD 50b, and (ii) twin-like parallel growths of staurolite and kyanite in Inner Schieferhülle schists GD 209a and GD 209b (fig. 3e). However, both textures could equally well be the result of simultaneous staurolite and kyanite growth, an explanation corroborated by the occurrence of kyanite within 100 m of the staurolite + biotite isograd (fig. 10). Staurolite and kyanite cannot be co-precipitated as the result of any discontinuous (Fe, Mg) reaction as both phases are highly aluminous; the only possible mechanism would be a continuous reaction of the form:



which could only operate in a KFMASH + 1 (or more) component system.

This textural study has shown that some (but not all) of the reactions leading to the development of the metapelite mineral assemblages can be equated with model univariant isograd reactions. The occurrence of good textural evidence for reaction D in schists of the gt + st + chl subzone and the abundance of texturally well-equilibrated ctd + biot schists together confirm that more than one sequence of reactions operated in south-east Tauern metapelites of similar AFM compositions.

### Discussion

The distribution of incompatible AFM mineral assemblages in the south-east Tauern could have one of two explanations:

(i) The three metamorphic zones and the gt + st + chl subzone represent distinct facies in P T space at fixed  $a_{\text{H}_2\text{O}}$  (as illustrated by fig. 11), so that the sequences of assemblages in the Mallnitz-Obervellach area (gt + chl, ctd + biot, st + biot) and the Kolbnitz area (gt + ctd + chl, gt + st + chl, st + biot) constitute different facies series (MIYASHIRO, 1961). In this case, it is assumed that the P T positions of the isograd reactions (A to E) are insensitive to variations in Ca or Mn content of the rocks, so that the P T position of the invariant point in fig. 11 is essentially fixed.

(ii) The gt + st + chl subzone and the ctd + biot zone are isofacial and developed isobarically at peak metamorphic temperatures intermediate between those operative in the gt + chl and st + biot zones. This explanation could only apply if the P T positions of the isograd reactions varied with Ca or Mn content of the rocks so that the position of the invariant point in fig. 11 moved to higher or lower pressures with varying bulk composition.

At present there is insufficient evidence to distinguish between the two explanations. Minerals in the gt + st + chl subzone schist GD 308c are very rich in Mn, suggesting that there may be grounds for suspecting the second. If the sec-

ond explanation is correct, however, the observed segregation of the ctd + biot schists from gt + st + chl schists (fig. 10) could only have arisen if bulk rock Ca or Mn varied systematically along strike in the pelitic units of the Mölltal Schieferhülle. Clearly some whole-rock chemical analyses must be obtained before this question is resolved.

In the absence of clear evidence to the contrary, it is assumed that explanation (i) is correct, with the corollary that the mineral assemblages in the Mölltal Schieferhülle metapelites record an isothermal pressure gradient at the thermal peak of Alpine metamorphism. There is no a priori evidence from the present study for which of the two facies series (Kolbnitz vs. Mallnitz-Obervellach) is the higher pressure type.

Both types of facies series can be identified in other metamorphic terrains. Many textbooks (e.g. WINKLER, 1979) imply that the Kolbnitz type is more common and that the assemblage gt + chl + musc is invariably broken down by reaction E. Nevertheless, ctd + biot assemblages have been recorded from several terrains, including Naxos (JANSEN and SCHUILING, 1976), New Mexico (HOLDAWAY, 1978), various parts of southern Switzerland (KRIGE, 1917; BOSARD, 1929; FREY, 1969; FOX, 1974, 1975) the Ardennes (CAPDEVILA, 1968) and Stonehaven, Scotland (HARTE, 1975; HARTE and HUDSON, 1980). Thus, despite WINKLER's (1979, p. 219) assertion that "earlier reports of this mineral pair have been shown to be incorrect", it would appear that the Mallnitz-Obervellach (Stonehavian) facies series is more common than is generally thought.

The Schreinemaker's bundle in fig. 11 forms a small part of the petrogenetic grid linking all stable invariant and univariant equilibria involving the common pelitic AFM phases: garnet, staurolite, chloritoid, biotite, cordierite, chlorite and aluminosilicate. It should be possible to orientate fig. 11 uniquely in P-T space knowing the stable topology of the whole grid. Unfortunately, opinion is divided as to what this is. All published grids agree that the invariant point [as, cord] is stable. The stability field of ctd + biot extends from [as, cord] to lower pressures in the grids of ALBEE, (1965) for conditions of  $P_{\text{H}_2\text{O}} \approx P_{\text{tot}}$ , HOSCHEK (1969), HARTE (1975) and HARTE and HUDSON (1979), but towards higher pressures in those of ALBEE (1965) for  $P_{\text{H}_2\text{O}} \approx 0.5 P_{\text{tot}}$ , KEPEZHINSKAS (1974), KEPEZHINSKAS and KLESTOV (1977) and KORIKOVSKII (1977). I favour the former configuration for the following reasons:

(i) As kyanite is the only aluminosilicate found in the south-east Tauern, [as, cord] must lie within the kyanite stability field. Schists containing andalusite, chloritoid and biotite, apparently in equilibrium have been recorded (ALBEE, 1972) implying that the ctd + biot field extends to lower pressures. This is supported by the coexistence of chloritoid and biotite in rocks which equilibrated close to the  $\text{Al}_2\text{SiO}_5$  triple point (HOLDAWAY, 1978).

(ii) In eastern Scotland ctd + biot assemblages are developed in the Stonehaven area, geographically situated between the type areas of Barrovian medi-



one-dimensional thermal model is insufficient to explain the observed range of Alpine metamorphic facies. One possible cause (probably not the only one) for such lateral inhomogeneity is that there were large-wavelength (10 km +) regional variations in the combined heat flow contribution from the underlying basement and mantle during the prograde part of the Alpine metamorphic cycle.

Few records of metapelite assemblages exist for other parts of the eastern Tauern Window. EXNER (1957) records the assemblage *ctd* + *ky* in schists on Klein Silberpfennig (locality A in fig. 13). Assemblages 3 and 4 occur immediately above the basement-cover interface in Grossarl Tal (locality B fig. 13). Staurolite and kyanite coexist in parts of the Silbereck Mulde (fig. 2) but apparently not with biotite (ANGEL, 1939; ANGEL and STABER, 1952). With these few constraints in mind, metamorphic zones have been tentatively extrapolated over the entire eastern Tauern (fig. 13). To a first approximation the staurolite + biotite isograd forms a closed loop enveloping the Hochalm Kern. The highest grade rocks occupy the core of a "thermal dome" which coincides with the area of highest basement elevation (CLIFF et al., 1971). A similar culmination occurs in the western Tauern in the Zillertal and Tuxer Alps where rare *st* + *biot* assemblages are also developed (HOERNES, 1973). The two are separated by

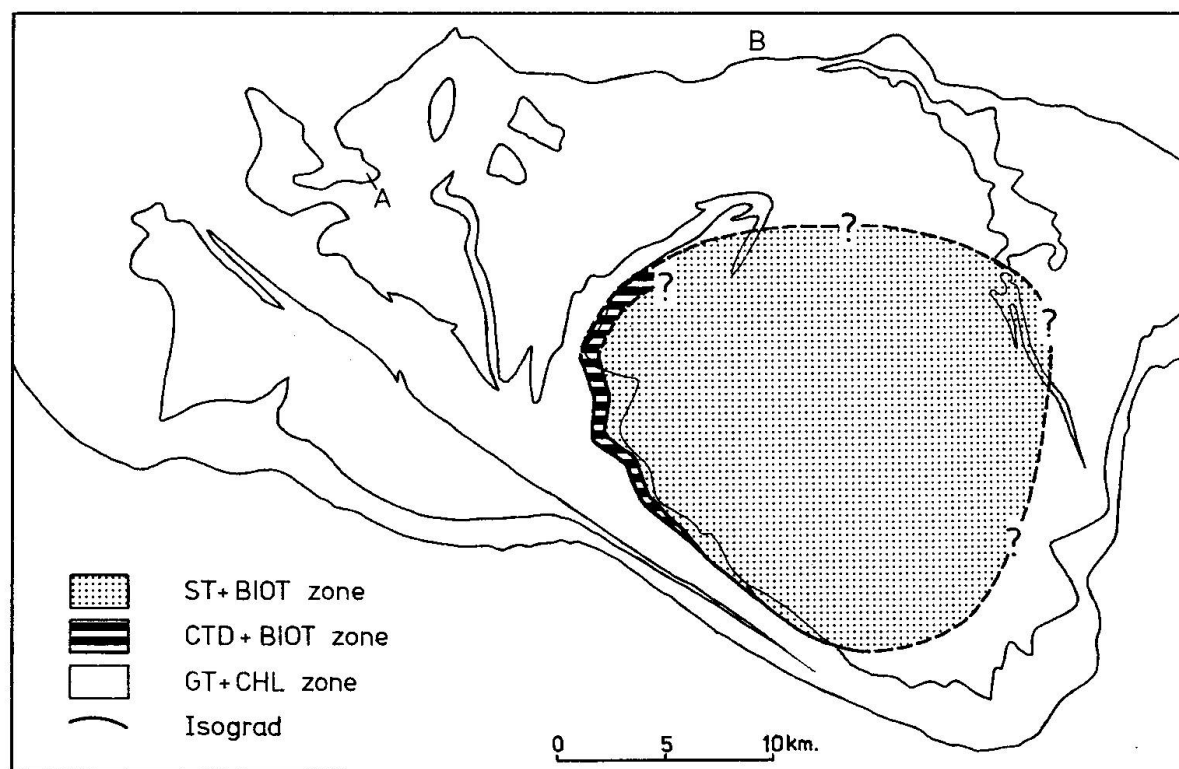


Fig. 13 Hypothetical metamorphic map of the eastern Tauern Window. A and B: Localities mentioned in the text.

the Glockner Depression, characterised by lower grade assemblages (CORNELIUS and CLAR, 1939; FRASL and FRANK, 1966). The coincidence of the "thermal dome" with the Hochalm Kern suggests that the latter was generated after the peak of Alpine metamorphism. The observation that the isograds are *not* folded round large  $D_a^2$  structures such as the Sonnblick Kern (DROOP, 1979) is consistent with a post- $D_a^2$  peak of metamorphism (fig. 5), and indicates that the gneiss-domes in the south-east Tauern were not all generated simultaneously.

### Conclusions

The conclusions of this paper can be summarised as follows:

1. Three Alpine metamorphic zones can be mapped in the metapelites of the south-east Tauern Window on the basis of AFM mineral assemblages:

(i) gt + chl zone; (ii) ctd + biot zone; (iii) st + biot zone.

The st + biot zone includes mainly structurally low rock units outcropping in the Hochalm Kern (the largest basement gneiss-dome in the E. Tauern), while the gt + chl zone covers mainly structurally high units exposed near the edge of the Window. The ctd + biot zone occurs between the two and appears to wedge out towards the south-east, where its place is taken by the gt + st + chl subzone in the highest grade part of the gt + chl zone.

2. The isograds separating the metamorphic zones can be modelled on a set of univariant reactions relating the phases garnet, chlorite, staurolite, chloritoid, biotite, muscovite, quartz and  $H_2O$ -rich fluid. Mg/Mg + Fe ratios of AFM minerals increase in the order: garnet  $\leq$  staurolite < chloritoid < biotite < chlorite.

3. The distribution of incompatible Alpine AFM mineral assemblages in the south-east Tauern Window indicates that metamorphic temperatures increased proceeding towards structurally lower units exposed in the Hochalm Kern. It also implies either (i) that an isothermal pressure gradient existed along the Mölltal at the thermal peak of Alpine metamorphism (with higher pressures towards the south-east), or (ii) that the pressure along any isotherm was essentially constant, but that the P T positions of the model isograd reactions used as a petrogenetic grid are highly sensitive to variations in bulk-rock concentrations of non-AFM components such as Ca or Mn.

4. Overdefined AFM mineral assemblages are common in Peripheral Schieferhülle schists sampled from close to isograds and in Inner Schieferhülle schists of the st + biot zone. Their presence could be due to one or more of the following: (i) the non-reactive nature of garnet; (ii) the presence of sufficient Ca or Mn to cause discontinuous (Fe, Mg) reactions to become continuous; (iii) buffering of pore fluid compositions by solid phases.



5. Mineral assemblages developed as the result of both continuous and discontinuous reactions. Some of the latter can be equated with the model univariant isograd reactions. More than one sequence of reactions operated in metapelites of similar AFM compositions.

6. Isograds (and hence, isotherms) rose through the Pennine rocks of the Tauern Window after major Alpine penetrative deformation had ceased, but were subsequently rotated together with foliation surfaces into steep attitudes near the southern margin of the Window as the result of late updoming centred on the Hochalm Kern.

7. Metapelites of the Inner Schieferhülle suffered pre-Alpine regional and contact metamorphism, but were extensively recrystallised during Alpine metamorphism.

#### Acknowledgements

This work has greatly benefited from discussions with E. R. Oxburgh, S. W. Richardson, T. J. B. Holland, P. C. England and B. Harte. G. A. Chinner and T. J. B. Holland are particularly thanked for constructive criticism of the manuscript. A research studentship from N. E. R. C. is gratefully acknowledged.

#### References

- ALBEE, A. L. (1965): A petrogenetic grid for the Fe-Mg silicates of pelitic schists. *Am. Jour. Sci.*, 263, p. 512-536.
- ALBEE, A. L. (1972): Metamorphism of pelitic schists: reaction relations of chloritoid and staurolite. *Geol. Soc. America Bull.*, 83, p. 3249-3268.
- ANGEL, F. (1940): Mineralfazien und Mineralzonen in den Ostalpen. *Jb. Univ. Graz.*, p. 251-304.
- ANGEL, F. and STABER, R. (1952): Gesteinswelt und Bau der Hochalm-Ankogel-Gruppe. *Wissenschaftliche Alpenvereinshefte*, 13, Universitätsverlag Wagner, Innsbruck, pp. 113.
- ATHERTON, M. P. (1977): The metamorphism of the Dalradian rocks of Scotland. *Scot. J. Geol.*, 13, p. 331-370.
- ATHERTON, M. P. and BROTHERTON, M. S. (1972): The composition of some kyanite-bearing regionally metamorphosed rocks from the Dalradian. *Scot. J. Geol.*, 8, p. 203-213.
- BARROW, G. (1912): On the geology of lower Dee-side and the southern Highland Border. *Proc. Geol. Ass.*, 23, p. 274-290.
- BESANG, C., HARRE, W., KARL, F., KREUZER, H., LENZ, H., MULDER, P and WENDT, I. (1968): Radiometrische Altersbestimmungen (Rb/Sr und K/Ar) an Gesteinen des Venediger-Gebietes (Hohe Tauern, Österreich). *Geol. Jb. (Hannover)*, 86., p. 835-844.
- BÉTHUNE, P. DE, LADURON, D. and BOQUET, J. (1975): Diffusion processes in resorbed garnets. *Contr. Mineral. and Petrol.*, 50, p. 197-204.
- BICKLE, M. J. and HAWKESWORTH, C. J. (1978): Deformation phases and the tectonic history of the eastern Alps. *Geol. Soc. America Bull.*, 89, p. 293-306.
- BICKLE, M. J., HAWKESWORTH, C. J., ENGLAND, P. C. and ATHEY, D. R. (1975): A preliminary thermal model for regional metamorphism in the Eastern Alps. *Earth Planet. Sci. Letters*, 26, p. 13-28.

- BOSSARD, L. (1929): Petrographie der mesozoischen Gesteine im Gebiete der Tessiner Kulmination. *SMPM*, 9, p. 107-159.
- BUTLER, B. C. M., (1967): Chemical study of minerals from the Moine schists of the Ardnamurchan area, Argyllshire, Scotland, *J. Pet.*, 8, p. 233-267.
- CAPDEVILA, M. R. (1968): Les types de metamorphisme "intermediaires de basse pression" dans le segment hercynien de Galice nord-orientale. *Comt. Rendu. Acad. Sci.*, 266, p. 1924-1927.
- CARMICHAEL, D. M. (1970): Intersecting isograds in the Whetstone Lake area, Ontario. *J. Petr.*, 11, p. 147-181.
- CHINNER, G. A. (1965): The kyanite isograd in Glen Clova, Angus, Scotland. *Min. Mag.*, 34, p. 132-143.
- CHINNER, G. A. (1978): Metamorphic zones and fault-displacement in the Scottish Highlands. *Geol. Mag.*, 115, p. 37-45.
- CIPRIANI, C., SASSI, F. P. and SCOLARI, A. (1971): Metamorphic white micas: definition of paragenetic fields. *SMPM*, 51, p. 259-302.
- Cliff, R. A. (1968): Geologic studies in the south-east corner of the Tauern Window, Austria. Unpublished D. Phil., thesis, Oxford.
- CLIFF, R. A. (1971): Strontium isotope distribution in a regionally metamorphosed granite from the Zentralgneiss, south-east Tauernfenster, Austria. *Contr. Mineral. and Petrol.*, 32, p. 274-288.
- CLIFF, R. A., NORRIS, R. J., OXBURGH, E. R. and WRIGHT, R. C. (1971): Structural metamorphic and geochronological studies in the Reisseck and southern Ankogel Groups, the Eastern Alps. *Jb. Geol. B-A., Wien*, 114, p. 121-272.
- CORNELIUS, H. P. and CLAR, E. (1939): Geologie des Grossglocknergebietes. *Abh. d. Rst. f. Bdf.*, 1, p. 1-305.
- DALLMEYER, R. D. (1974): Metamorphic history of the northeastern Reading Prong, New York and northern New Jersey. *J. Pet.*, 15, p. 325-359.
- DROOP, G. T. R. (1979): Metamorphic studies in the south-east Tauern Window, Austria. Unpublished D. Phil. thesis, Oxford. pp. 357.
- ENGLAND, P. C. (1978): Some thermal considerations of Alpine metamorphism - past, present and future. *Tectonophysics*, 46, p. 21-40.
- ENGLAND, P. C. and RICHARDSON, S. W. (1977): The influence of erosion upon the mineral facies of rocks from different metamorphic environments. *J. Geol. Soc. London*, 134, p. 201-213.
- EVANS, B. W. and GUIDOTTI, C. V. (1965): The sillimanite-potash feldspar isograd in Western Maine, USA. *Contr. Mineral. and Petrol.*, 12, p. 25-62.
- EXNER, C. (1957): Erläuterungen zur geologischen Karte der Umgebung von Gastein. *Geol. B-A., Wien*, 168 pp.
- EXNER, C. (1962): Sonnblicklamelle und Molltallinie. *Jb. Geol. B-A., Wien*, p. 273-286.
- EXNER, C. (1964): Erläuterungen zur geologischen Karte der Sonnblickgruppe. *Geol. B-A., Wien*, 170 pp.
- FOX, J. S. (1974): Petrology of some low-variance metapelites from the Lukmanier Pass area, Switzerland. Unpublished Ph. D. thesis, Cambridge. 220 pp.
- FOX, J. S. (1975): Three dimensional isograds from the Lukmanier Pass, Switzerland, and their tectonic significance. *Geol. Mag.*, 112, p. 547-564.
- FRASL, G. and FRANK, W. (1966): Einführung in die Geologie und Petrographie im Tauernfenster. *Der Augschluss*, 15, p. 30-58.
- FREY, M. (1969): Die Metamorphose des Keupers vom Tafeljura bis zum Lukmaniergebiet. *Beitr. Geol. Schweiz., n. F.* 137, 160 pp.
- FREY, M. (1974): Alpine metamorphism of pelitic and marly rocks of the Central Alps. *SMPM.*, 54, p. 489-508.
- GANGULY, J. (1968): Analysis and stability of chloritoid and staurolite and some equilibria in the system  $\text{FeO-Al}_2\text{O}_3\text{-SiO}_2\text{-H}_2\text{O-O}_2$ . *Am. Jour. Sci.*, 266, p. 277-298.



- GANGULY, J. and NEWTON, R. C. (1968): Thermal stability of chloritoid at high pressure and relatively high oxygen fugacity. *J. Pet.*, 9, p. 444-466.
- GRANT, J. A. and WEIBLEN, P. W. (1971): Retrograde zoning in garnet near the second sillimanite isograd. *Am. Jour. Sci.*, 270, p. 281-296.
- GREENWOOD, H. J. (1975): Buffering of pore fluids by metamorphic reactions. *Am. Jour. Sci.*, 275, p. 573-593.
- HALFERDAHL, L. B. (1961): Chloritoid: its composition, X-ray and optical properties, stability and occurrence. *J. Pet.*, 2, p. 49-135.
- HARTE, B. (1975): Determination of a pelite petrogenetic grid for the Eastern Scottish Dalradian. *Carnegie Inst. Wash. Yr. B.*, 74, p. 438-446.
- HARTE, B. and HUDSON, N. F. C. (1979): Pelite facies and the temperatures and pressures of metamorphism in E. Scotland, p. 323-337 in *The Caledonides of the British Isles - reviewed*. Ed. HARRIS, A. L., HOLLAND, C. H. and LEAKE, B. E. The Geological Society, London.
- HARTE, B. and JOHNSON, M. R. W. (1969): Metamorphic history of Dalradian rocks in Glen Clova, Esk and Lethnot, Angus, Scotland. *Scot. J. Geol.*, 5, p. 54-80.
- HAWKESWORTH, C. J. (1976): Rb/Sr geochronology in the Eastern Alps. *Contr. Mineral. and Petrol.*, 54, p. 225-244.
- HAWKESWORTH, C. J., WATERS, D. J. and BICKLE, M. J. (1975): Plate tectonics in the Eastern Alps. *Earth Planet. Sci. Letters*, 24, p. 405-413.
- HEY, M. H. (1954): A new review of the chlorites. *Min. Mag.*, 30, p. 277-292.
- HOERNES, S. (1973): Untersuchungen zur Metamorphose in den westlichen Hohen Tauern (Österreich). *Tschermaks Min. Pet. Mitt.*, 20, p. 81-106.
- HOLDAWAY, M. J. (1978): Significance of chloritoid-bearing and staurolite-bearing rocks in the Picuris range, New Mexico. *Geol. Soc. America Bull.*, 89, p. 1404-1414.
- HOLLAND, T. J. B. (1979): High water activities in the generation of high pressure kyanite eclogites of the Tauern Window, Austria. *J. Geol.*, 87, p. 1-27.
- HOLLISTER, L. S. (1969): Contact metamorphism in the Kwoiek area of British Columbia: an end-member of the metamorphic process. *Geol. Soc. America Bull.*, 80, p. 2465-2494.
- HOSCHEK, G. (1967): Untersuchungen zum Stabilitätsbereich von Chloritoid und Staurolith. *Contr. Mineral. and Petrol.*, 14, p. 123-162.
- HOSCHEK, G. (1969): The stability of staurolite and chloritoid and their significance in the metamorphism of pelitic rocks. *Contr. Mineral. and Petrol.*, 22, p. 208-232.
- HOUNSLOW, A. W. and MOORE, J. M. (1967): Chemical petrology of Grenville schists near Fernleigh, Ontario. *J. Pet.*, 8, p. 1-28.
- JANSEN, J. B. H. and SCHUILING, R. D. (1976): Metamorphism on Naxos: petrology and geothermal gradients. *Am. Jour. Sci.*, 276, p. 1225-1253.
- JÄGER, E., KARL, F. and SCHMIDEGG, O. (1969): Rubidium-Strontium-Altersbestimmungen an Biotit-Muscovit-Granitgneisen (Typus Augen- und Fasergneiss) aus dem nördlichen Grossvenedigerbereich (Hohe Tauern). *Tschermaks Mineral. Petrog. Mitt.*, 13, p. 251-272.
- KEPEZHINSKAS, K. B. (1973): Pressure variability during medium temperature metamorphism of metapelites. *Lithos*, 6, p. 145-158.
- KEPEZHINSKAS, K. B. and KHLESTOV, V. V. (1977): The petrogenetic grid and subfacies for middle-temperature metapelites. *J. Pet.*, 18, p. 114-148.
- KORIKOVSKII, S. P. (1979): Metamorphic facies of metapelites. Academic Press, Moscow (in Russian).
- KRIGE, L. J. (1917): Petrographische Untersuchungen in Val Piora und Umgebung. *Eclogae Geol. Helv.*, 14, p. 519-654.
- LAMBERT, R. ST. J. (1964): Isotopic age determinations on gneisses from the Tauernfenster. *Verh. Geol. B.-A., Wien*, p. 16-27.
- MELSON, W. G. (1966): Phase equilibria in calc-silicate hornfels, Lewis and Clark County, Montana. *Am. Mineral.*, 51, p. 402-421.

- MILLER, CH. (1974): On the metamorphism of eclogites and high-grade blue-schists from the Penninic terrain of the Tauern Window, Austria. *SMPM*, 54, p. 371–384.
- MILLER, CH. (1977): Chemismus und phasenpetrologische Untersuchungen der Gesteine aus der Eclogitzone des Tauernfenster, Österreich. *Tschermaks Min. Petr. Mitt.*, 24, p. 221–277.
- MIYASHIRO, A. (1961): Evolution of metamorphic belts. *J. Pet.*, 2, p. 277–311.
- NARÁY-SZABÓ, I. and SASVÁRI, K. (1958): On the structure of staurolite,  $HFe_2Al_9Si_4O_{24}$ . *Acta Cryst.*, 11, p. 862–865.
- OXBURGH, E. R. and TURCOTTE, D. L. (1974): Thermal gradients and regional metamorphism in overthrust terrains with special reference to the Eastern Alps. *SMPM*, 54, p. 641–662.
- RICHARDSON, S. W. (1968): Staurolite stability in parts of the system Fe-Al-Si-O-H. *J. Pet.*, 9, p. 467–488.
- RUMBLE, D. (1974): Silicate, sulfide and oxide mineral paragenesis of the Clough Formation, Black Mountain, New Hampshire. *EOS. Trans. Am. Geophys. Union (abstract)*, 55, p. 449.
- SATIR, M. (1974): Rb-Sr-Altersbestimmungen an Glimmern der westlichen Hohen Tauern. Interpretation und Geologische Bedeutung, *SMPM*, 54, p. 213–228.
- SWEATMAN, J. R. and LONG, J. V. P. (1969): Quantitative electron-probe micro-analysis of rock-forming minerals. *J. Pet.*, 10, p. 322–379.
- THOMPSON, A. B., LITTLE, P. T. and THOMPSON, J. B. (1977a): Mineral reactions and A-Na-K and A-F-M facies types in the Gassetts Schists, Vermont. *Am. Jour. Sci.*, 277, p. 1124–1151.
- THOMPSON, A. B., TRACY, R. J., LITTLE, P. T. and THOMPSON, J. B. (1977b): Prograde reaction histories deduced from compositional zonation and mineral inclusions in garnet from the Gassetts Schists, Vermont. *Am. Jour. Sci.*, 277, p. 1152–1167.
- THOMPSON, J. B. (1957): The graphical analysis of mineral assemblages in pelitic schists. *Am. Mineral.*, 42, p. 842–858.
- TILLEY, C. E. (1925): A preliminary survey of metamorphic zones in the southern Highlands of Scotland. *Q. J. Geol. Soc. London*, 81, p. 100–112.
- TRACY, R. J., ROBINSON, P. and THOMPSON, A. B. (1976): Garnet composition and zoning in the determination of temperature and pressure of metamorphism, central Massachusetts. *Am. Mineral.*, 61, p. 762–775.
- TROMMSDORFF, V. (1968): The Wollastonite reaction in the Western Bergell Alps. *SMPM.*, 48, p. 828–829.
- TROMMSDORFF, V. (1972): Change in T-X during metamorphism of siliceous dolomitic rocks of the Central Alps. *SMPM.*, 52, p. 567–571.
- VELDE, B. and RUMBLE, D. (1977): Alumina content of chlorite in muscovite-bearing assemblages. *Carnegie Inst. Wash. Yr. B.*, 76, p. 621–623.
- WINKLER, H. G. F. (1979): Petrogenesis of metamorphic rocks. Springer-Verlag, New York. 5th Edition, 348 pp.
- ZEN, E.-AN. (1966): Construction of pressure-temperature diagrams for multicomponent systems after the method of Schreinermakers – a geometric approach. *Bull. U.S. Geol. Surv.*, 1225.
- ZWART, H. J. (1963): Some examples of the relations between deformation and metamorphism from the central Pyrenees. *Geol. Mijnbouw*, 42, p. 143–154.